Accepted Manuscript

Synthesis and biological evaluation of 2,6-disubstituted-*9H*-purine, 2,4-disubstitued-thieno[3,2-*d*]pyrimidine and -*7H*-pyrrolo[2,3-*d*]pyrimidine analogues as novel CHK1 inhibitors

Zifei Han, Chao Tian, Yuanxin Li, Meng Wang, Jiajia Yang, Xiaowei Wang, Zhili Zhang, Junyi Liu

PII: S0223-5234(18)30319-2

DOI: 10.1016/j.ejmech.2018.03.075

Reference: EJMECH 10340

To appear in: *European Journal of Medicinal Chemistry*

Received Date: 8 February 2018

Revised Date: 14 March 2018

Accepted Date: 26 March 2018

Please cite this article as: Z. Han, C. Tian, Y. Li, M. Wang, J. Yang, X. Wang, Z. Zhang, J. Liu, Synthesis and biological evaluation of 2,6-disubstituted-*9H*-purine, 2,4-disubstitued-thieno[3,2-*d*]pyrimidine and -*7H*-pyrrolo[2,3-*d*]pyrimidine analogues as novel CHK1 inhibitors, *European Journal of Medicinal Chemistry* (2018), doi: 10.1016/j.ejmech.2018.03.075.

Graphic Abstract

Synthesis and biological evaluation of 2,6-disubstituted-*9H*-purine, 2,4-disubstitued-thieno[3,2-*d*]pyrimidine and -*7H*-pyrrolo[2,3-*d*]pyrimidine analogues as novel CHK1 inhibitors

Zifei Han, [1,†] Chao Tian, [1,*] Yuanxin Li, Meng Wang, Jiajia Yang, Xiaowei Wang, Zhili Zhang, Junyi Liu [*]

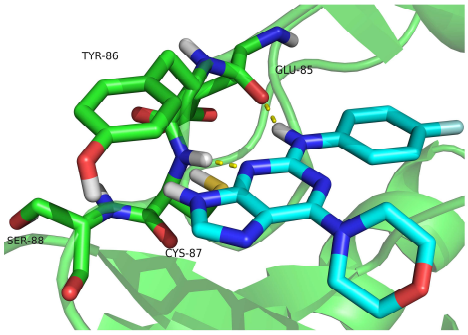

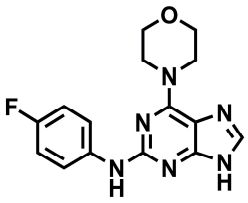

3l

CHK1 IC_{50} : 0.684 μM

HT29 GI_{50} >100 μM

HEK293 GI_{50} >100 μM

Potentiation factor: 7.0

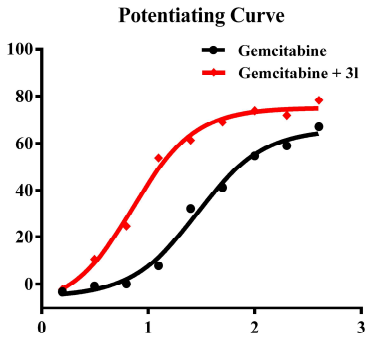

Synthesis and biological evaluation of 2,6-disubstituted-*9H*-purine, 2,4-disubstitued-thieno[3,2-*d*]pyrimidine and -*7H*-pyrrolo[2,3-*d*]pyrimidine analogues as novel CHK1 inhibitors

Zifei Han,[1,†] *Chao Tian,*[1,*,†] *Yuanxin Li,*[†] *Meng Wang,*[†] *Jiajia Yang,*[†] *Xiaowei Wang,*[†] *Zhili Zhang,*[†] *Junyi Liu*[*,†,‡]

[†] Department of Chemical Biology, School of Pharmaceutical Sciences, Peking University, Beijing 100191, China

[‡] State Key Laboratory of Natural and Biomimetic Drugs, Peking University, Beijing 100191, China

[1] Co-first author of this paper. These authors contributed equally.

[*]Co-corresponding author of this paper. Chao Tian: tianchao@bjmu.edu.cn; Junyi Liu: jyliu@bjmu.edu.cn.

ABSTRACT

Checkpoint kinase 1 (CHK1) inhibitors can potentiate the effectiveness of deoxyribonucleic acid (DNA) damaging agents in the treatment of cancer. A novel series of 2,6-disubstituted-*9H*-purine (**3a-p**, **5a** and **5b**), 2,4-disubstituted-thieno[3,2-*d*]pyrimidine (**8a-c**) and 2,4-disbustituted-*7H*-pyrrolo[2,3-*d*]pyrimidine (**11a-c**) analogues were designed and synthesized as potent CHK1 inhibitors. Compounds (**3a**, **3d**, **3f** and **3j-l)** with *9H*-purine core displayed more potent inhibition against CHK1. The most potent compound (**3l**) also exhibited low anti-proliferative effects towards HT29 and Hek293 cell lines. In addition, **3l** showed strong potentiating effect (7-fold) on the anti-proliferative activity of gemcitabine towards HT29 cells. The results of cell cycle assay indicated that **3l** could strikingly affect the cell cycle distribution of the gemcitabine-treated HT29 cells and induce a significant S phase accumulation. The kinase selectivity profile of **3l** displayed acceptable selectivity against other kinases. These results rendered **3l** a potent lead compound of CHK1 inhibitor for further investigation.

KEYWORDS

CHK1 inhibitors, *9H*-Purine, Potentiating effect, Anti-proliferative effects.

1. INTRODUCTION

Cell cycle is well controlled by cell cycle checkpoints, which are indispensable in the growth and survival of normal cells as well as tumor cells. In response of the DNA damage resulting from cytotoxic agents or ionizing radiation [1, 2], the cell cycle checkpoints will be activated to induce the cell cycle arrest at corresponding phase and subsequently recruit the factors involving in the DNA damage repair mechanism. Checkpoint kinase 1 (CHK1) plays an essential role in the S-phase and G2/M-phase cell cycle checkpoints and DNA damage response in cells [3]. CHK1 is a serine-threonine kinase. It is mainly phosphorylated and activated by its upstream kinase ATR (Ataxia Telangiectasia-Mutated and Rad3-related) in response to single strand breaks in DNA. After phosphorylated on residues Ser-317 and Ser-345 of CHK1, an auto-phosphorylation takes place on residue Ser-296 to obtain the activated CHK1 [4, 5]. A number of downstream proteins including cell division cycle 25 (Cdc25) family are phosphorylated by the activated CHK1 and finally regulate the cell cycle progression. Furthermore, the repair of damaged DNA was also promoted by CHK1 through signaling to the repair protein RAD51 [6].

As we know that nearly half of the tumor cells are *p53*-defficient ones, which results in an absence of G1 arrest in cell cycle checkpoints. Based on the crucial role of CHK1 in the cell cycle checkpoints and DNA damage repair mechanism especially for these *p53*-mutant tumors, CHK1 has been considered as an excellent target of antitumor agents with potentiating effect. A number of reports had confirmed that selective inhibition of CHK1 with small molecules, or inactivation by RNA interference (RNAi) could enhance the effectiveness of chemotherapy or ionizing radiation therapy **[7]**. After the discovery of the first CHK1 inhibitor, UCN-01 (7-hydroxystaurosporine) [8, 9], plenty of compounds were reported as potent CHK1 inhibitors

[10]. Some of these compounds, including AZD7762 [11], MK-8776 [12], PF477736 [13], LY2603618 [14], Prexasertib (LY2606368) [15, 16], GDC-0425 [17] and CCT245737 [18, 19], entered the clinical trials in combination with chemotherapeutic agents. However, only the clinical trials concerning LY2606368 and CCT245737 are still active on the ClinicalTrials.gov recently. Most of the others were terminated for toxicity and severe side effects [20-22].

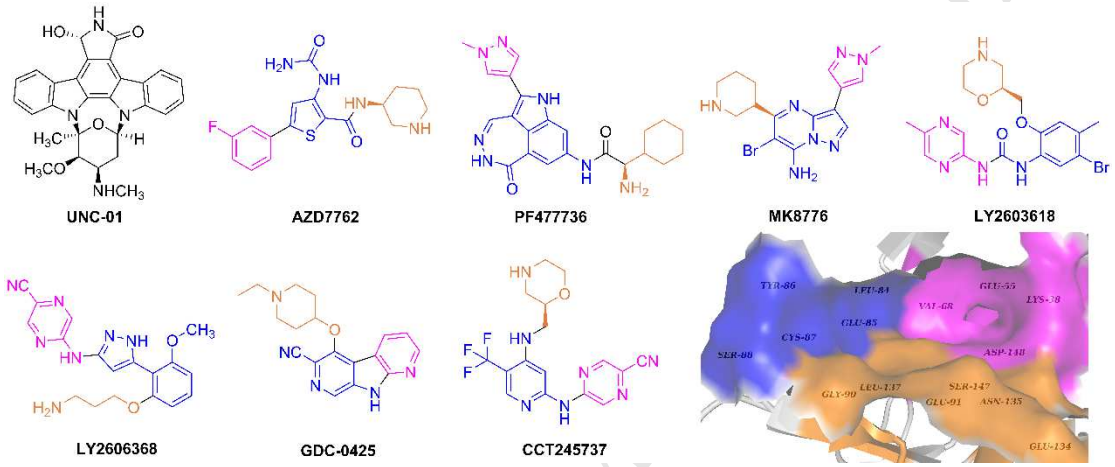

Figure 1. The representative CHK1 inhibitors and the ATP-binding site of CHK1

As shown in **Figure 1**, the structures of the CHK1 inhibitors are diverse and can be generally divided into three fragments (blue, orange and purple) according to the corresponding crystal structures of the inhibitors bound to the adenosine triphosphate (ATP)-binding site of CHK1. The "blue fragments" always bound to the "hinge region" of the ATP-binding site of CHK1 which was generally formed by Glu-85, Tyr-86, Cys-87 and Ser-88 residues. The "orange fragments" always bound to the "ribose region" which was formed by Gly-90, Glu-91, Glu-134, Asn-135 and Leu-137 residues. The "purple fragments" usually bound to the "interior pocket" which was formed by Lys-38, Glu-55, Val-68, Leu-84 Ser-147 and Asp-148 residues. When the inhibitors bound to the ATP-binding site of CHK1, the "blue fragments" of the inhibitors were in charge of

"pushing" the other two fragments into their corresponding binding sites. These three fragments were indispensable in the scaffold of CHK1 inhibitors.

As we know that fused bicyclic pyrimidine derivatives played an important role in the discovery of kinases inhibitors [23-27]. Replacement of pyrimidine with purine or pyrrolopyrimidine was also reported to bring many advantages in the biological activities and pharmacokinetic profiles of kinase inhibitors [28]. In a previous study, 6-morpholino-*9H*-purine was reported as a CHK1 inhibitor with an IC_{50} value of micromole [29].The absence of the "interior pocket" binding fragment (purple) was considered as a key reason of low inhibitory activity of 6-morpholino-*9H*-purine against CHK1. Based on the reported structure-activity relationships of CHK1 inhibitors, we thought that introduction of substituted (hetero)aromatic amine group on position 2 of 6-morpholino-*9H*-purine was conducive to enhancing its potency in CHK1 inhibition and potentiating effect. Taking the 6-morpholino-*9H*-purine and the "interior pocket" binding fragments of CHK1 inhibitors together, in this work, we designed a series of 2,6-disubstituted-*9H*-purine as novel CHK1 inhibitors (**Figure 2**). A range of substituted (hetero)aromatic amines on position 2 were investigated to evaluated the effect of the "interior pocket" binding fragments on this scaffold. As a contrast, several 2-substituted-*N*-(tetrahydro-*2H*-pyran-4-yl)-*9H*-purin-6-amines, 2,4-disubstituted-thieno[3,2-*d*]pyrimidines and 2,4-disubstituted-*7H*-pyrrolo[2,3-*d*]pyrimidines were also synthesized to further investigate the effect of the 6-morpholino-*9H*-purine backbone structure on the potency of CHK1 inhibition. The inhibition against CHK1 and anti-proliferation toward HT29 and Hek293 cells of the target compounds were evaluated to discovery potent CHK1 inhibitors with low cytotoxicities. Furthermore, the potentiating effect on gemcitabine-induced

cell proliferation inhibition, the effect on the cell cycle distribution and kinase selectivity profile of the most potent compound were further estimated.

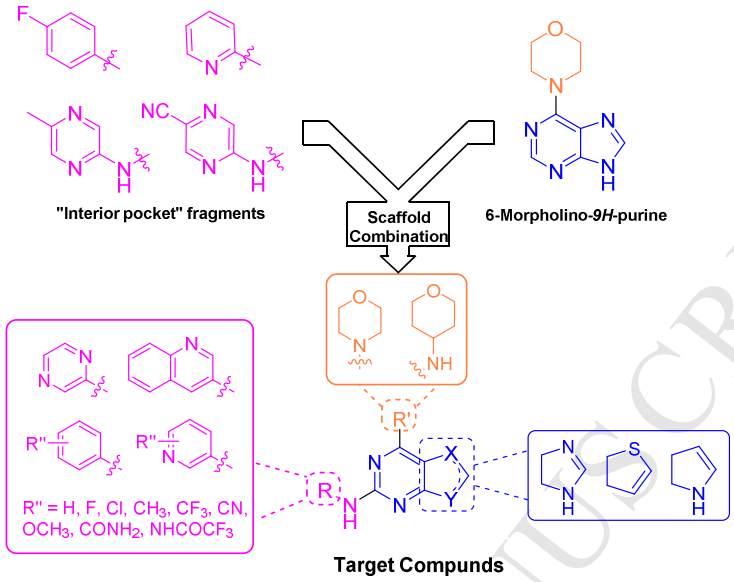

Figure 2. Design of the novel CHK1 inhibitors

2. RESULTS AND DISCUSSIONS

2.1. Synthesis of target compounds

The target compounds were synthesized using 2,6-dichloro-*9H*-purine (**1**), 2,4-dichlorothieno[3,2-*d*]pyrimidine (**6**) and 2,4-dichloro-*7H*-pyrrolo[2,3-*d*]pyrimidine (**9**) as the row material. The synthetic route was outlined in **Scheme 1**. Firstly, morpholine group was introduced to the 4- or 6-position of the dichloro derivatives (**1**, **6** and **9**) through refluxing in the presence of trimethylamine in ethanol (EtOH) for 10 h to obtain 2-chloro-6-morpholin-4-yl-*9H*-purine (**2**), 2-chloro-4-morpholin-4-yl-thieno[3,2-*d*]pyrimidine (**7**) and 2-chloro-4-morpholin-4-yl-*7H*-pyrrolo[2,3-*d*]pyrimidine (**10**). A similar reaction was conducted between 2,6-dichloro-*9H*-purine and 4-aminotetrahydropyran to achieve 2-chloro-*N*-(tetrahydro-*2H*-pyran-4-yl)-*9H*-purin-6-amine (**4**). Subsequently, the target compounds **3a-p**, **5a**, **5b**, **8a-c** and **11a-c** were assembled via a microwave assisted amination of compounds **2,**

4, 7 and **10** with different (hetero)aromatic amines ($ArNH_2$) catalyzing by trifluoroacetic acid (TFA) or palladium(II) acetate ($Pd(OAc)_2$) [30, 31].

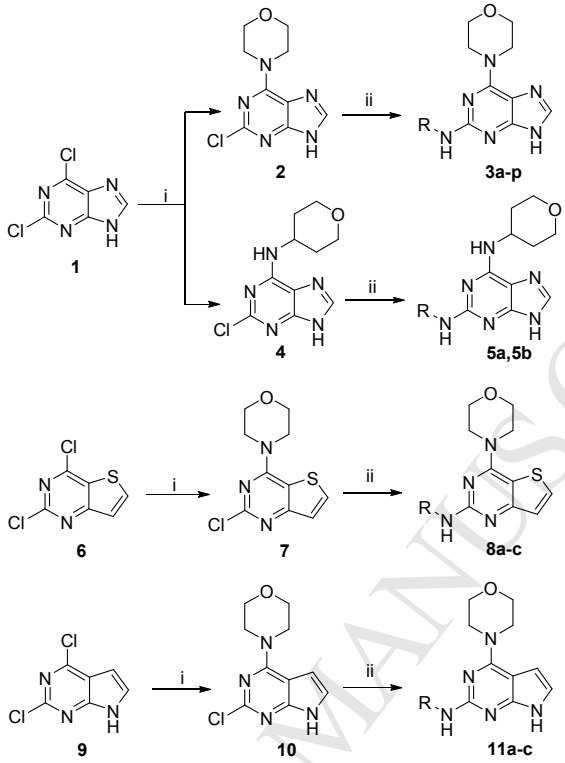

Scheme 1. The synthesis route of compound **3a-p**, **5a**, **5b**, **8a-c** and **11a-c**

Reagents and conditions: i. Morpholine (or 4-aminotetrahydropyran), trimethylamine, EtOH, reflux; ii. $ArNH_2$, TFA, 2,2,2-trifluoroethanol (CF_3CH_2OH), microwave, 140 ºC, 1.5h. or $ArNH_2$, $Pd(OAc)_2$, 4,5-bis(diphenylphosphino)-9,9-dimethylxanthene (Xantphos), caesium carbonate (Cs_2CO_3), microwave, 160 ºC, 40 min.

2.2. Biological evaluation

2.2.1. CHK1 kinase inhibition

The inhibitory activities of these compounds in the concentration of 10 μM against CHK1 were evaluated using ADP-Glo kit and listed in **Table 1**. The thieno[3,2-*d*]pyrimidine analogues **8a-c** had no inhibition against CHK1. In contrast to *7H*-pyrrolo[2,3-*d*]pyrimidines **11a-c**, *9H*-purine analogues **3a-c** exhibited moderate to high potency in CHK1 inhibition. From the results of **3a-c,**

8a-c and **11a-c**, a sequence of potencies in CHK1 inhibition could be summarized as follow: *9H*-purine analogues > *7H*-pyrrolo[2,3-*d*]pyrimidine analogues >> thieno[3,2-*d*]pyrimidine analogues. These results implied that 7-*N* of *9H*-purine might bring some interactions with CHK1 to promote the inhibitory activities. *9H*-purine is more suitable to be the backbone structure of CHK1 inhibitors. Furthermore, **3a** displayed 82.4% (10 μM) inhibition against CHK1. However, the inhibitory activity of its 4-aminotetrahydropyran analogue **5a** was only 61.5%. This indicated that morpholine group had better directly "connect" to the 6-position of *9H*-purine. This could also be demonstrated by the inhibitory activities of **3l** and **5b**.

Our main interests in this work were focusing on the substituent groups on 2-*NH* of 6-morpholino-*9H*-purine. From the results of **3a-p**, we could summarize some structure-activity relationships as follow. As the inhibition activity of **3c** was lower than **3b**, it seemed that multi-substituted phenyl group on 2-*NH* would reduce the inhibition against CHK1. From the inhibitory activities of **3b** (*p*-OCH_3), **3d** (*m*-OCH_3) and **3e** (*o*-OCH_3), we could find that the substituted position on 2-aminophenyl will significantly affect the inhibition against CHK1. The sequence of inhibitory activities is *m*- > *p*- >> *o*-. To further investigate the effect of the substituents, a range of substituents were introduced to *m*-position of phenyl such as -OCH_3, -CH_3, -CF_3, -OCF_3, -Cl and -F to generate **3d** and **3f-k**. Among them, *m*-F substituted analogue (**3k**) was the best one, exhibiting 92.0% inhibition against CHK1. Besides, inhibition activities of *m*-OCH_3 and *m*-CH_3 analogues (**3d** and **3f**) were also more than 80%. Beyond our expectation, *p*-F substituted analogue **3l** also exhibited strong potency in CHK1 inhibition, though a little lower than that of the *m*-substituted analogue (**3k**). The above results indicated that small volume and

strong electro-withdraw groups on phenyl were conductive to the inhibitory activity. The effect of the former (volume) was predominant.

Furthermore, three other heteroaromatic rings were introduced to 2-*NH* of 6-morpholino-9*H*-purine to generate compounds **3m** (3'-pyridinyl), **3o** (3'-quinolinyl) and **3p** (2'-pyrazinyl). As the order of inhibitory activities were **3a** ≥ **3m** > **3p** > **3o**, phenyl and pyridinyl ring were undoubtedly the best two aromatic rings on 2-*NH* of 6-morpholino-9*H*-purine. Moreover, compound **3n** displayed more than 80% inhibition against CHK1.

Table 1. The inhibitory activities of target compounds against CHK1

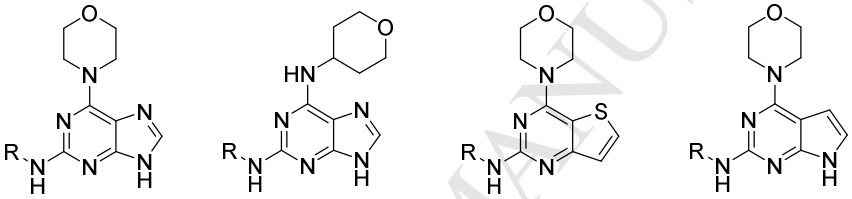

No.	R	Inhibition against CHK1 at 10 μM (CHK1 IC_{50} (μM))	No.	R	Inhibition against CHK1 at 10 μM (CHK1 IC_{50} (μM))
3a		82.4% (2.57)	**3n**	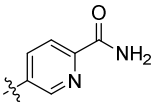	80.3% (9.87)
3b	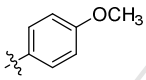	51.0%	**3o**		38.2%
3c	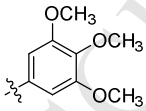	35.8%	**3p**	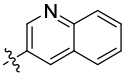	63.1%
3d	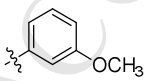	84.9% (3.63)	**5a**		61.5%
3e	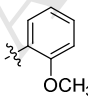	3.8%	**5b**	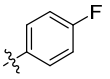	37.2%
3f	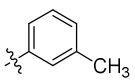	85.2% (1.27)	**8a**		N.D.
3g	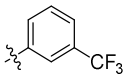	61.3%	**8b**	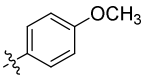	N.D.

3h	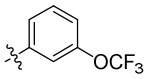	31.6%	**8c**	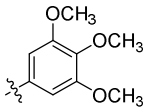	N.D.
3i	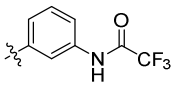	50.0%	**11a**		44.5%
3j	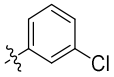	77.3% (2.83)	**11b**	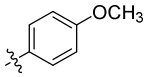	16.7%
3k	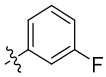	92.0% (3.60)	**11c**	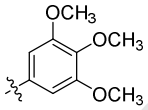	26.9%
3l	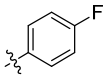	89.9% (0.684)	**AZD7762**		0.006
3m		82.2% (8.06)	**CCT245737**		0.002

Compounds **3a**, **3d**, **3f**, 3**j-l**, **3m** and **3n**, which displayed more than 75% inhibition against CHK1, were selected to further determine their IC_{50} values. AZD7762 and CCT245737 were used as the positive controls. Compounds **3a**, **3d**, **3f**, **3j** and **3k** with substituted phenyl groups on 2-*NH* exhibited moderate inhibitory activities against CHK1, ranging from 1.27 to 3.63 μM. The pyridinyl analogues **3m** and **3n** displayed low potencies in CHK1 inhibition (8.06 and 9.87μM). These results indicated that substituted phenyl groups as substituents on 2-*NH* of 6-morpholino-*9H*-purine were better than pyridinyl groups in this scaffold. Despite weaker than AZD7762 and CCT245737, compound **3l** with an IC_{50} value of 0.684 μM showed the strongest potency in inhibition of CHK1 among our target compounds.

2.2.2. Anti-proliferative effect toward HT29 cells and Hek293 cells

The anti-proliferative effects of target compounds were assessed on the HT29 cell line (*p*53-mutant), which were presented in **Table 2**. The positive controls, AZD7762 and CCT245737,

showed moderate to strong potencies in anti-proliferation against HT29 cells, with GI_{50} values of 0.167 and 9.223 μM, respectively. However, most of our target compounds exhibited low anti-proliferative potencies on HT29 cells. Among them, the GI_{50} values of compounds **3a**, **3c**, **3e**, **3h**, **3l**, **3m** and **3o** were all above 100 μM, which indicated extremely low anti-proliferative effect toward HT29 cells.

Table 2. The GI_{50} values (μM) of target compounds toward HT29 and Hek293 cells

No.	HT29 GI_{50} (μM)	Hek293 GI_{50} (μM)	No.	HT29 GI_{50} (μM)	Hek293 GI_{50} (μM)
3a	>100	60.2	**3n**	72.2	72.2
3b	74.5	>100	**3o**	>100	27.2
3c	>100	>100	**3p**	25.1	22.3
3d	72.6	38.7	**5a**	80.3	31.5
3e	>100	>100	**5b**	86.9	>100
3f	67.6	40.5	**8a**	54.5	>100
3g	29.1	31.4	**8b**	29.7	>100
3h	>100	>100	**8c**	31.6	>100
3i	58.0	73.6	**11a**	58.3	64.7
3j	34.8	38.4	**11b**	38.4	63.6
3k	60.8	33.7	**11c**	50.4	58.7
3l	>100	>100	**AZD7762**	0.167	0.236
3m	>100	33.7	**CCT245737**	9.223	1.387

As low cytotoxicity is necessary for CHK1 inhibitors, all the target compounds were also assessed their anti-proliferative activities toward Hek293 cell line. As shown in **Table 2**, AZD7762 and CCT245737 exhibited strong anti-proliferative effects on Hek293 cells with GI_{50} values of 0.236 and 1.387 μM, respectively. Contrastingly, our compounds displayed low to moderate potencies in anti-proliferation on Hek293 cells. To our delight, the most potent **3l** showed nearly no anti-proliferative potency toward Hek293 cells (GI_{50} > 100 μM). The lower anti-proliferative activity of **3l** implied higher safety profile in drug combination.

2.2.3. Colony formation assay

In order to guide the subsequent antitumor potentiation assay, the colony formation assay was performed to further assess the cytotoxicity of **3l** on HT29 cell line. HT29 cells (100 cells per well) was treated by different concentrations of **3l** ranging from 100 nM to 100 μM for 2 weeks. As shown in **Figure 3**, **3l** did not significantly affect the colony formation of HT29 cells when the concentration of **3l** was no higher than 10 μM. Therefore, in the subsequent potentiation assay, no more than 10 μM of **3l** would be used in combination with gemcitabine in HT29 cells.

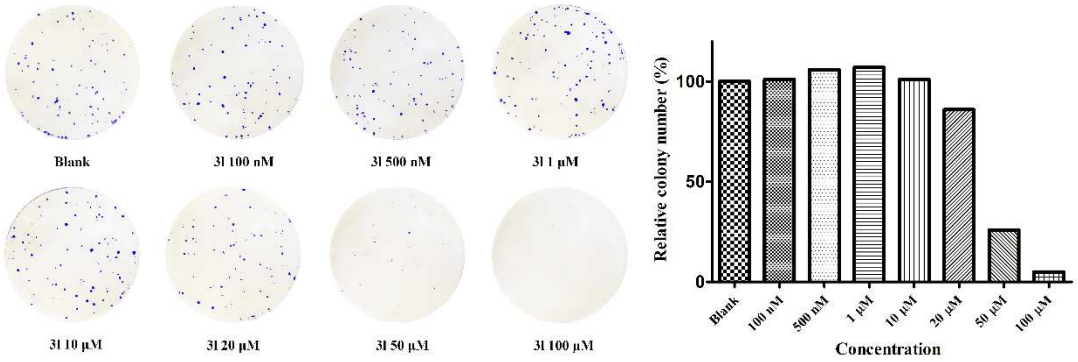

Figure 3. The effect of **3l** on the colony formation of HT29 cells.

2.2.4. Antitumor potentiation assay

To evaluate the antitumor potentiating effect of **3l** to DNA-damaging agents, the concentration-response of HT29 cells to proliferation inhibition by gemcitabine (GEM, ranging from 1.5 nM to 400 nM) was measured with or without **3l** (10 and 1 μM). AZD7762 (50 nM) was used as the positive control. The ratio of GI_{50} value of GEM alone over that of GEM in combination with CHK1 inhibitor was set as potentiation factor (PF) to estimate the anti-tumor potentiating effect of CHK1 inhibitor [32].

As shown in **Figure 4** and **Table 3**, the GI_{50} value of GEM was 105.9 nM toward HT29 cells. The potentiating effect of **3l** was dependent on its concentration. Lower concentration of **3l** (1 μM) did not enhance the anti-proliferation of GEM significantly. However, in combination with 10 μM of **3l**, the GI_{50} value of GEM strikingly reduced to 15.2 nM (PF = 7.0), displaying a strong potentiating effect. Although, the PF value of **3l** was less than that of AZD7762 (PF = 15.8), the potentiation assay demonstrated compound **3l** as a good CHK1 inhibitor possessed a strong potentiating effect to GEM in HT29 cells.

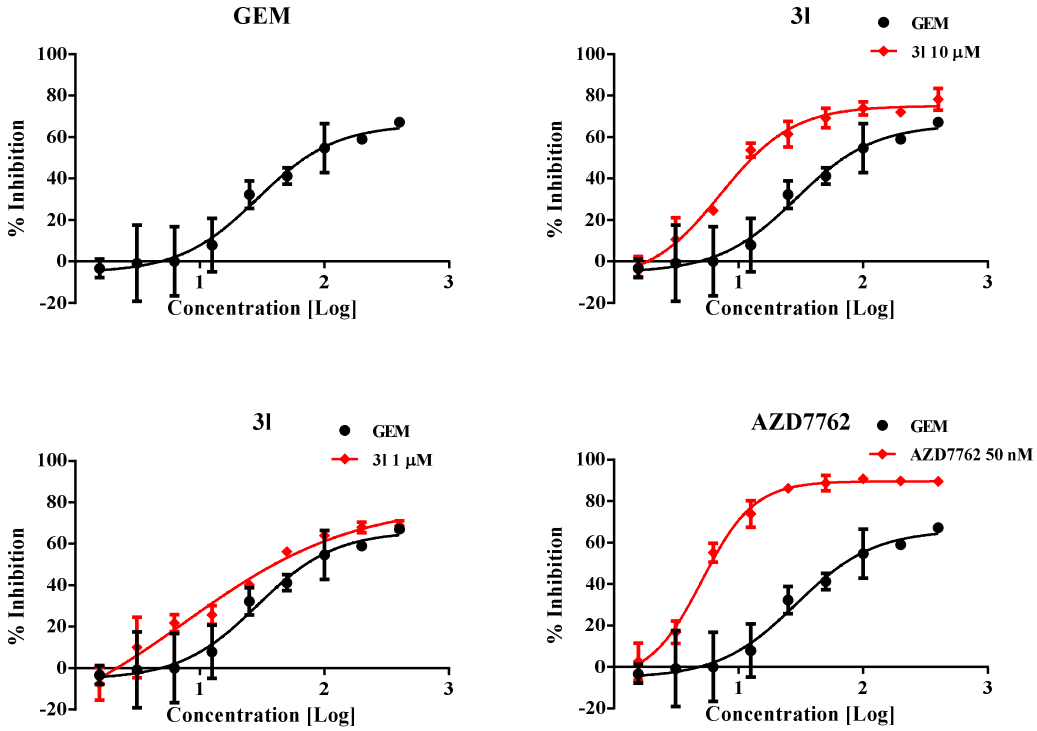

Figure 4. Anti-proliferation curve of GEM in the presence of **3l** and AZD7762. The black curves in all four plots were anti-proliferative curves of GEM. In contrast, the red curves were the anti-proliferative curve of GEM in combination with **3l** (10 and 1 μM) or AZD7762 (50 nM).

Table 3. Potentiation effects of **3l** and AZD7762 to GEM in HT29 cells.

	GI_{50} (nM)	PF[a]
GEM	**105.9**	
GEM+3l (10 μM)	**15.2**	**7.0**
GEM+3l (1 μM)	**54.4**	**1.9**

GEM+AZD7762	**6.7**	**15.8**

a. Potentiation factor = ratio of GI_{50} value of GEM alone over that of GEM in combination with **3l** (10 μM and 1 μM) or AZD7762 (50 nM).

2.2.5. Cell cycle distribution

The cell cycle assay was performed to further study the effect of **3l** on the cell cycle distribution. HT29 cells were treated by **3l** alone, GEM alone and GEM in combination with **3l**, respectively. As shown in **Figure 5** and **6**, in contrast to the untreated control, there was no obvious change in the cell cycle distribution of HT29 cells after treated by 10 μM of **3l**. This was in consistent with the low anti-proliferation inhibition of **3l**. After treated by 25 nM of GEM, the percentage of G2/M phase cells increased from 7.0% (blank) to 85.2%, indicating a significant G2/M arrest. However, after treated by GEM in combination with 10 μM of **3l**, the population of G2/M phase cells reduced from 85.2% to 25.2%, meanwhile, the S phase increased from 30.9% to 61.0%. The above results indicated that compound **3l** could induce a significant S phase accumulation in the GEM treated HT29 cells. This result was in line with the previous report on the cell cycle profiles of CHK1 inhibitors in combination with GEM in HT29 cells, in which a similar S phase accumulation was observed in the HT29 cells after treated by GEM plus a CHK1 inhibitor (CHIR-124) [33].

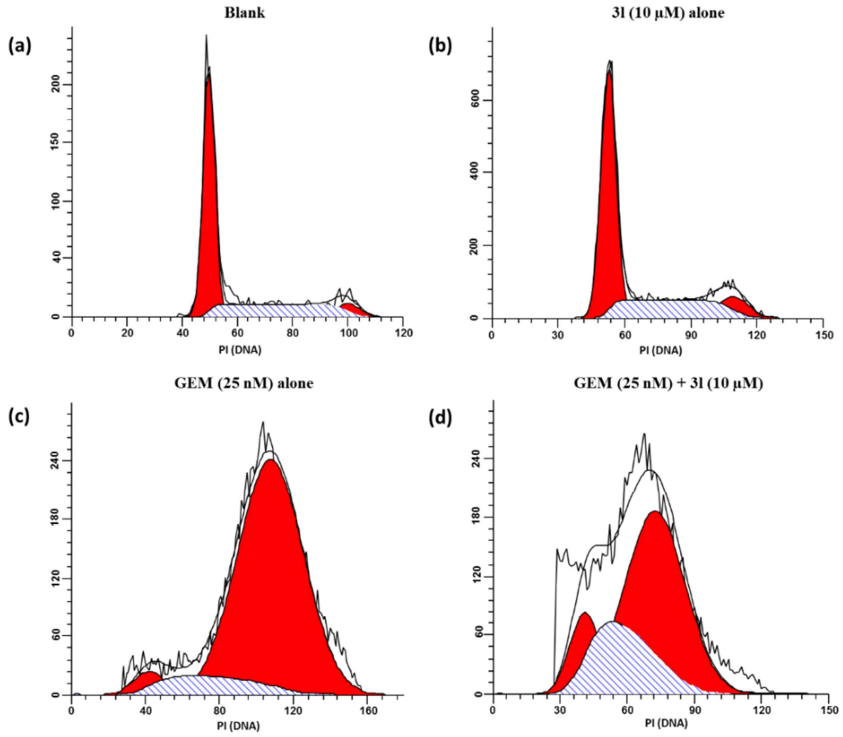

Figure 5. Cell cycle distributions of HT29 cells after treated by **3l** (10 μM) alone, GEM alone and GEM plus **3l** (10 μM) in relative to untreated control. **a**. untreated control; **b**. **3l** (10 μM) alone; **c**. GEM (25 nM) alone; **d**. GEM (25 nM) in combination with **3l** (10 μM).

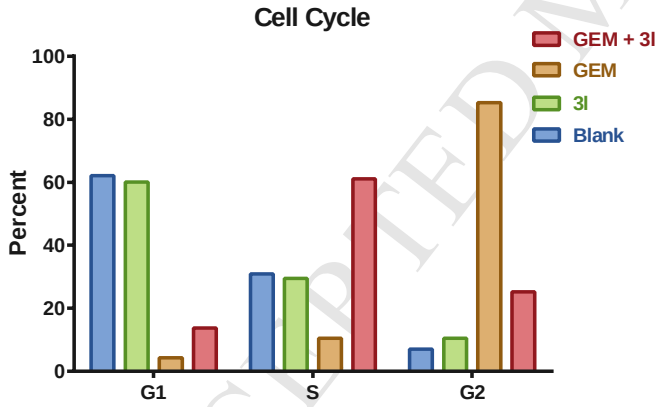

	Blank	3l	GEM	GEM +3l
G1	62.1%	60.0%	4.3%	13.8%
S	30.9%	29.5%	10.5%	61.0%
G2	7.0%	10.5%	85.2%	25.2%

Figure 6. Histogram of cell cycle distributions of HT29 cells treated by **3l**, GEM and GEM in combination with **3l**, respectively.

2.2.6. Kinase selectivity assay

The kinase inhibitory activities of **3l** were also determined against fourteen crucial kinases from six different kinase families at higher concentration of 10 μM. The inhibition results were

illustrated in **Figure 7.** At concentration of 10 μM, **3l** exhibited nearly 90% inhibition toward CHK1. Besides, it also displayed 72% and 73% inhibition against Checkpoint kinase 2 (CHK2) and Cyclin-dependent kinase 2 (CDK2). Moreover, the inhibitory activities of **3l** were all less than 50% against the other 11 kinases. Especially for calcium/calmodulin-dependent protein kinase type IV (CAMK4), RAC-alpha serine/threonine-protein kinase (AKT1), catalytic subunit α of protein kinase A (PKAC-α), Anaplastic lymphoma kinase (ALK) and epidermal growth factor receptor (EGFR) kinases, **3l** displayed nearly no inhibitory activities. These results indicated that **3l** possessed reasonable kinase selectivity toward CHK1 over the other kinases. Nevertheless, more work should be done to optimize the structures of our compounds to reduce the inhibitory activities against CHK2 and CDK2.

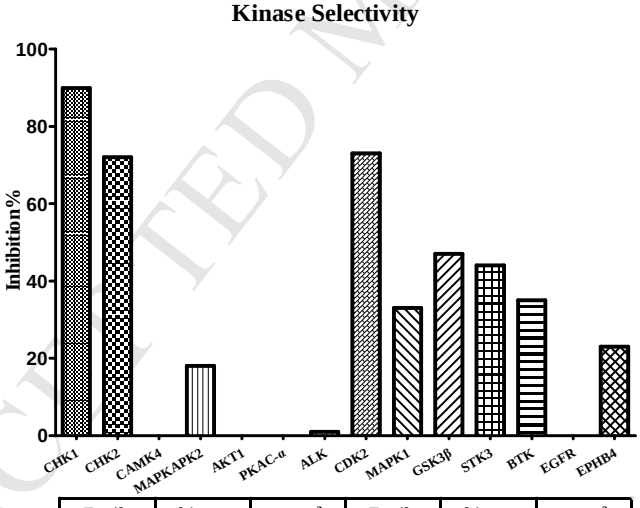

Family	kinase	Inh% [a]	Family	kinase	Inh% [a]
CAMK Family	CHK1	89.9	CMGC Family	CDK2	73.0
	CHK2	72.0		MAPK1	33.0
	CAMK4	0.0		GSK3β	47.0
	MAPKAPK2	18.0	STE Family	STK3	44.0
AGC Family	AKT1	0.0	TK Family	BTK	35.0
	PKAC-α	0.0		EGFR	0.0
TKL Family	ALK	1.0		EPHB4	23.0

a Inh% is short for Inhibition%

Figure 7. Histogram and table of kinase selectivity profile of **3l** against representative kinases. 14 kinases from six different kinase families were selected to determine their inhibition by **3l** at the concentration of 10 μM.

2.3. Molecular modeling study

A molecular modeling study was performed on compound **3l** using a reported crystal structure of CHK1 (PDB: 5F4N) [18]. As shown in **Figure 8**, the binding mode of **3l** indicated that the purine structure could form two hydrogen bonds with Glu-85 and Cys-87 residues at the hinge area. However, the hydrogen-bonding interactions in the ribose region and interior pocket were not obvious. Furthermore, the *p*-F-phenyl group and purine ring of **3l** formed a big planar structure. The interior pocket was filled with the *p*-F-phenyl group on 2-*NH* of **3l**. Bulky substituents were unfavorable to the pocket. This was consistent with our biological assay result that smaller substituted groups on phenyl ring of 2-*NH* was conducive to the potency on CHK1 inhibition. The stretching of morpholine group of **3l** into the ribose region was obstructed by Glu-91 residue. The flexibility of the substituent on position 6 of purine should be reconsidered. This modeling result revealed that purine was a good backbone structure of CHK1 inhibitor and more appropriate substituent groups on position 2 and 6 should be further investigated.

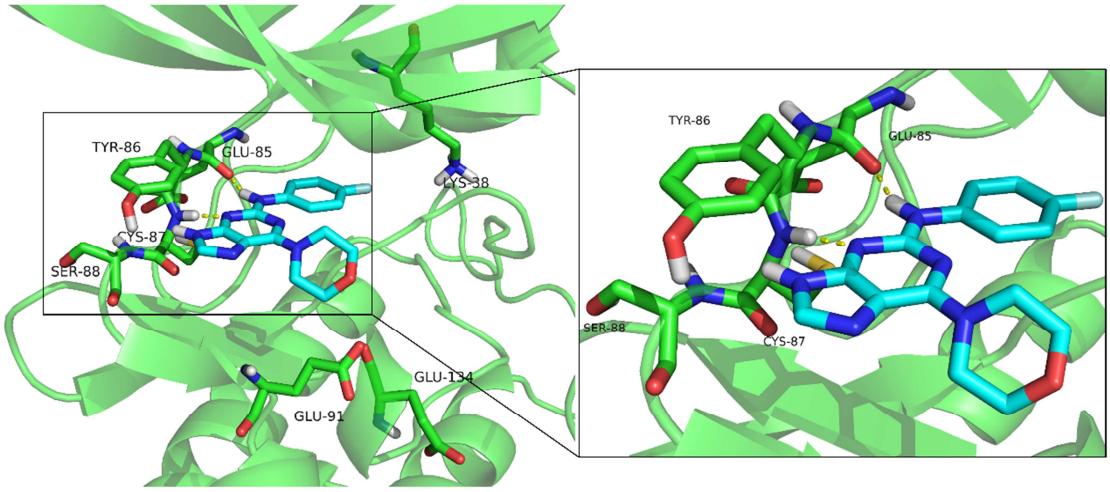

Figure 8. Predicting docking mode of **3l** with the crystal structure of CHK1 (5F4N). Compound **3l** was displayed in cyan. Hydrogen bonds between **3l** and amino acid residue of CHK1 were indicated with dashed lines in yellow.

3. CONCLUSION

A series of 2,6-disubstituted-*9H*-purine, 2,4-disubstituted-thieno[3,2-*d*]pyrimidine and -*7H*-pyrrolo[2,3-*d*]pyrimidine analogues were synthesized as novel CHK1 inhibitors. Among the three types of compounds, purine analogues possessed the best potency in CHK1 inhibition. 2,6-Disubstituted-*9H*-purine analogues **3a**, **3d**, **3f** and **3j-n** displayed good inhibitory activities against CHK1. Among them, **3l** with an IC_{50} of 0.684 μM was undoubtedly the best one. Furthermore, compound **3l** exhibited nearly no anti-proliferative activity toward HT29 and Hek293 cells, which implied a good safety profile. The antitumor potentiating assay showed that **3l** could significantly lower the gemcitabine GI_{50} from 105.9 nM to 15.2 nM. In addition, **3l** could strikingly affect the cell cycle distribution of the gemcitabine treated HT29 cells and induce a significant S phase accumulation. Kinase selectivity assay revealed that **3l** displayed acceptable selectivity toward 14 kinases. All above results rendered **3l** a good lead compound of CHK1 inhibitors for further investigation. A series of **3l** analogues varied at 6-position are under synthesis to discover more potent CHK1 inhibitors.

4. EXPERIMENTAL SECTION

4.1. Chemistry

4.1.1. General information

All the reagents and solvents were purchased from common commercial suppliers without further purification. Microwave assisted reactions were performed on the Discovery SP (CEM, USA). Melting points (m.p.) were determined using a SGW X4 apparatus. Mass spectra were recorded on MDS SCIEX QSTAR system. ^{1}H- and ^{13}C-NMR spectra were recorded with a Varian INOVA-400

or INOVA-600 with dimethyl sulfoxide-d_6 (DMSO-d_6) as solvent. Tetramethylsilane (TMS) was used as an internal standard to express the chemical shift in ppm (parts per million): s, singlet; bs, broad singlet; d, doublet; t, triplet; q, quartet; quin, quintet m, multiplet; and bs, broad singlet. IR spectra were recorded on a Nicolet-6700 FT-IR spectrometer (KBr pellets). Thin-layer chromatography (TLC) with a fluorescent indicator was utilized to monitor the reaction progress, and the spots were visualized under 254 and 365 nm illumination. All test compounds were assessed for purity by Agilent Technologies 1260 Infinity HPLC system. HPLC condition: methanol (CH_3OH): H_2O = 60:40; flow rate, 1.0 mL/min; UV detection, from 220 to 365 nm; temperature, ambient; injection volume, 20 μL. The purity of all the test compounds was greater than 95%.

4.1.2. General procedure for synthesis of compounds 2, 4, 7 and 10

A suspension of 300mg of 2,6-dichloro-*9H*-purine (**1**), 2,4-dichlorothieno[3,2-*d*]pyrimidine (**6**) or 2,4-dichloro-*7H*-pyrrolo[2,3-*d*]pyrimidine (**9**) in 10 mL of EtOH was added morpholine or 4-aminotetrahydropyran (1.2 equiv) and 300μL of triethylamine. The mixtrue was refluxed for 10 hours. After the disappearance of compounds **1**, **6** or **9** detected by TLC, the solution was evaporated in vacuum to yield a syrup. Then, it was neutralized by concentrated ammonium hydroxide. After filtering off, the residue was washed with cold water and cold acetone successively to remove the triethylammonium hydrochloride.

4.1.2.1. 4-(2-chloro-9H-purin-6-yl)morpholine (2)

Compound **2** was obtained as a white solid (yield 80.8%). m.p. >300 ºC; ^{1}H NMR (400 MHz,

DMSO-d_6) δ: 3.72 (s, 4H, CH_2NCH_2), 4.18 (bs, 4H, CH_2OCH_2), 8.16 (s, 1H, C*H*), 13.23 (s, 1H, 9-N*H*); ^{13}C NMR (100 MHz, DMSO-d_6) δ: 46.0, 66.5, 118.2, 139.4, 152.9, 153.1, 153.8; MS (ESI): $[M+H]^+$: 240.10. IR (KBr pellet, cm^{-1}): 3437, 3099, 2976, 2832, 1581, 1450, 1359, 1315, 1277, 1262, 1160, 1116, 1032, 959, 940, 833, 636, 524.

4.1.2.2. 2-chloro-N-(tetrahydro-2H-pyran-4-yl)-9H-purin-6-amine (4)

White solid. m.p. 151-152 ºC; ^{1}H NMR (400 MHz, DMSO-d_6) δ: 1.68 (s, 2H, CH_2CHCH_2) , 1.79 (s, 2H, CH_2CHCH_2), 3.40 (s, 2H, CH_2OCH_2), 3.88 (s×2, 2H, CH_2OCH_2), 4.21 (bs, 1H, NHC*H*), 8.13 (s, 2H, N*H* and C*H*), 13.08 (s, 1H, 9-N*H*); ^{13}C NMR (100 MHz, DMSO-d_6) δ: 19.0, 32.6, 33.6, 46.7, 66.6, 105.0, 118.2, 139.8, 151.0, 153.4, 154.6; MS (ESI): $[M+H]^+$: 254.09. IR (KBr pellet, cm^{-1}): 3431, 3128, 2971, 2874, 2602, 2519, 2101, 1587, 1520, 1497, 1474, 1450, 1437, 1375, 1299, 1238, 1229, 1206, 1186, 1169, 1080, 1032, 1017, 1001, 988, 952, 905, 869, 856, 767, 655, 636, 556, 484, 418.

4.1.2.3. 4-(2-chlorothieno[3,2-d]pyrimidin-4-yl)morpholine (7)

Compound **7** was obtained as a white solid (yield 72.3 %). m.p. 193-194 ºC; ^{1}H NMR (400 MHz, DMSO-d_6) δ: 3.71-3.80 (m, 4H, CH_2NCH_2), 3.87-3.96 (m, 4H, CH_2OCH_2), 7.41 (d, J = 5.5 Hz, 1H, C*H*), 8.31 (d, J = 5.5 Hz, 1H, SC*H*); ^{13}C NMR (100 MHz, DMSO-d_6) δ: 46.4, 66.3, 113.0, 124.2, 135.9, 156.4, 158.7, 163.2; MS (ESI): $[M+H]^+$: 256.15. IR (KBr pellet, cm^{-1}): 3096, 3080, 2997, 2967, 2904, 2856, 2773, 1545, 1518, 1488, 1448, 1431, 1367, 1291, 1275, 1242, 1183, 1133, 1114, 1045, 1017, 945, 925, 872, 826, 791, 732, 700, 648, 606, 525.

4.1.2.4. 4-(2-chloro-7H-pyrrolo[2,3-d]pyrimidin-4-yl)morpholine (10)

Compound **10** was obtained as a white solid (yield 75.4 %). m.p. 259-260 ºC; ^{1}H NMR (400 MHz, DMSO-d_6) δ: 3.72 (s, 4H, CH_2NCH_2), 3.83 (s, 4H, CH_2OCH_2), 6.66 (s, 1H, C*H*), 7.21 (s, 1H, NHC*H*), 11.92 (s, 1H, 7-N*H*); ^{13}C NMR (100 MHz, DMSO-d_6) δ: 45.8, 66.4, 101.1, 101.9, 122.5, 152.3, 153.3, 157.4; MS (ESI): $[M+H]^+$: 239.13. IR (KBr pellet, cm^{-1}): 3192, 3114, 2985, 2969, 2895, 2860, 1590, 1569, 1487, 1450, 1439, 1374, 1346, 1322, 1295, 1274, 1253, 1167, 1141, 1120, 1022, 955, 903, 874, 832, 797, 729, 718, 680, 630, 596, 528.

4.1.3. General procedure for microwave assisted introduction aromatic amine on position 2 of compound 2, 4, 7 and 10.

***General procedure A to obtain compounds 3a-l, 5a, 5b, 8a-c, 11a-c*:** to a stirred suspension of 50 mg 2-cholro analogues **1**, **4**, **6** or **9** (1 equiv) and aromatic amine (2 equiv) in 2 ml of 2,2,2-trifluoroethanol (TFE) was added TFA (40 µl) dropwise. The reagents were placed in a sealed microwave vial and the reactions were performed under microwave irradiation (140 ºC for 90 min). The solvent was removed in vacuo and the residue was re-dissolved in dichloromethane (CH_2Cl_2) (10mL). The solution was washed with saturated sodium bicarbonate solution (3 × 10 mL), and the aqueous extracts were combined and washed with CH_2Cl_2 (10mL). The combined organic layers were dried with sodium sulfate anhydrous (Na_2SO_4). The solvent was removed under reduced pressure and the crude material was purified by column chromatography on silica gel.

***General procedure B to obtain compounds 3m-p*:** 4-(2-chloro-9*H*-purin-6-yl)morpholine

(50mg, 0.21mmol), heteroaromatic amine (1.2 equiv), 2 mol % $Pd(OAc)_2$, 3 mol % Xantphos, Cs_2CO_3 (140mg, 0.43mmol) in dioxane (1.5 mL) was heated to 160 °C in a microwave reactor for 40min. The solvent was removed under reduced pressure and the crude material was purified by column chromatography on silica gel with CH_2Cl_2/CH_3OH in a 15:1 (v/v) ratio as eluent, to afford product **3m-p**.

4.1.3.1. 6-morpholino-N-phenyl-9H-purin-2-amine (3a)

White solid, yield 81.1%. m.p. 271-272 ºC; ^{1}H NMR (400 MHz, DMSO-d_6) δ: 3.68-3.77 (m, 4H, CH_2NCH_2), 4.06-4.34 (m, 4H, CH_2OCH_2), 6.86 (t, J = 7.2 Hz, 1H, Ph-H4'), 7.23 (t, J = 7.8 Hz, 2H, Ph-H3', Ph-H5'), 7.76 (d, J = 8.0 Hz, 2H, Ph-H2', Ph-H6'), 7.85 (s, 1H, CH), 8.89 (s, 1H, 2-NH), 12.59 (s, 1H, 9-NH); ^{13}C NMR (100 MHz, DMSO-d_6) δ: 45.6, 66.7, 114.7, 118.7, 120.6, 128.8, 136.5, 142.1, 153.5, 153.8, 156.1; HRMS (ESI): calcd for $C_{15}H_{16}N_6O$ $[M+H]^+$: 297.1464, found: 297.1464. IR (KBr pellet, cm^{-1}): 3371, 3105, 2987, 2960, 2868, 1607, 1570, 1531, 1474, 1463, 1453, 1441, 1426, 1393, 1374, 1329, 1290, 1267, 1239, 1154, 1111, 1074, 1018, 937, 827, 786, 756, 731, 692, 638, 518.

4.1.3.2 N-(4-methoxyphenyl)-6-morpholino-9H-purin-2-amine (3b)

White solid, yield 80.3%, m.p. 231-232 ºC; ^{1}H NMR (400 MHz, DMSO-d_6) δ: 3.71 (bs, 7H, OCH_3, CH_2NCH_2), 4.18 (s, 4H, CH_2OCH_2), 6.83 (d, J = 8.7 Hz, 2H, Ph-H3', Ph-H5'), 7.63 (d, J = 8.6 Hz, 2H, Ph-H2', Ph-H6'), 7.81 (s, 1H, CH), 8.67 (s, 1H, 2-NH), 12.51 (s, 1H, 9-NH); ^{13}C NMR (100 MHz, DMSO-d_6) δ: 45.6, 55.6, 66.7, 114.0, 114.6, 120.5, 135.3, 136.2, 153.6, 153.8, 153.9, 156.4; HRMS (ESI): calcd for $C_{16}H_{18}N_6O_2$ $[M+H]^+$: 327.1569, found: 327.1574. IR (KBr

pellet, cm^{-1}): 3307, 2999, 2963, 2903, 2834, 1600, 1577, 1513, 1476, 1444, 1392, 1317, 1299, 1284, 1268, 1240, 1173, 1154, 1114, 1070, 1034, 937, 884, 831, 811, 785, 685, 626, 556, 525.

4.1.3.3. 6-morpholino-N-(3,4,5-trimethoxyphenyl)-9H-purin-2-amine (3c)

White solid, yield 70.3%. m.p. >300 ºC; ^{1}H NMR (400 MHz, DMSO-d_6) δ: 3.60 (s, 3H, OCH_3), 3.73 (m, 4H, CH_2NCH_2), 3.75 (s, 6H, OCH_3× 2), 4.20 (s, 4H, CH_2OCH_2), 7.18 (s, 2H, Ph-*H*2', Ph-*H*6'), 7.87 (s, 1H, C*H*), 8.78 (s, 1H, 2-N*H*), 12.54 (s, 1H, 9-N*H*); ^{13}C NMR (100 MHz, DMSO-d_6) δ: 49.1, 56.1, 60.6, 66.6, 96.4, 114.6, 131.8, 136.7, 138.3, 153.0, 153.4, 153.8, 156.0; HRMS (ESI): calcd for $C_{18}H_{22}N_6O_4$ $[M+H]^+$: 387.1781, found: 387.1774. IR (KBr pellet, cm^{-1}): 3422, 3280, 2960, 1602, 1584, 1509, 1484, 1453, 1432, 1398, 1354, 1110, 937, 879, 786, 622, 470.

4.1.3.4. N-(3-methoxyphenyl)-6-morpholino-9H-purin-2-amine (3d)

White solid, yield 76.2%. m.p. 209-210 ºC; ^{1}H NMR (400 MHz, DMSO-d_6) δ: 3.73 (s, 7H, OCH_3, CH_2NCH_2), 4.20 (s, 4H, CH_2OCH_2), 6.44 (d, J = 7.5 Hz, 1H, Ph-*H*4'), 7.11 (dd, J = 7.5, 8.0 Hz, 1H, Ph-*H*2'), 7.26 (d, J = 8.0 Hz, 1H, Ph-*H*5'), 7.57 (s, 1H, Ph-*H*6'), 7.86 (s, 1H, C*H*), 8.89 (s, 1H, 2-N*H*), 12.60 (s, 1H, 9-N*H*); ^{13}C NMR (100 MHz, DMSO-d_6) δ: 45.6, 55.3, 66.7, 104.4, 106.0, 111.7, 114.7, 129.4, 136.6, 143.3, 153.4, 153.8, 156.0, 160.0; HRMS (ESI): calcd for $C_{16}H_{18}N_6O_2$ $[M+H]^+$: 327.1569, found: 327.1566. IR (KBr pellet, cm^{-1}): 3380, 3178, 3003, 2900, 2858, 1605, 1577, 1493, 1439, 1412, 1374, 1306, 1291, 1267, 1215, 1158, 1107, 1025, 939, 870, 833, 785, 773, 729, 695, 632, 515, 459.

4.1.3.5. N-(2-methoxyphenyl)-6-morpholino-7H-purin-2-amine (3e)

White solid, yield 77.4%. m.p. 220-221 ºC; ^{1}H NMR (400 MHz, DMSO-d_6) δ: 3.73 (d, J = 4.1 Hz, 4H, CH_2NCH_2), 3.88 (s, 3H, OCH_3), 4.18 (s, 4H, CH_2OCH_2), 6.88 - 6.96 (m, 2H, Ph-H3', Ph-H5'), 7.00 (d, J = 5.6 Hz, 1H, Ph-H4'), 7.41 (s, 1H, Ph-H6'), 7.87 (s, 1H, CH), 8.42 (bs, 1H, 2-NH), 12.64 (s, 1H, 9-NH); ^{13}C NMR (100 MHz, DMSO-d_6) δ: 45.7, 56.2, 66.7, 110.8, 115.0, 118.4, 120.8, 121.3, 130.3, 136.7, 148.0, 153.4, 153.9, 155.7; HRMS (ESI): calcd for $C_{16}H_{18}N_6O_2$ $[M+H]^+$: 327.1569, found: 327.1573. IR (KBr pellet, cm^{-1}): 3434, 2967, 2856, 1601, 1579, 1537, 1490, 1457, 1435, 1410, 1312, 1288, 1265, 1243, 1217, 1177, 1158, 1113, 1024, 937, 887, 834, 784, 741, 632, 563, 519.

4.1.3.6. 6-morpholino-N-(m-tolyl)-9H-purin-2-amine (3f)

White solid, yield 83.8%. m.p. 181-182 ºC; ^{1}H NMR (400 MHz, DMSO-d_6) δ: 2.27 (s, 3H), 3.73 (s, 4H, CH_2NCH_2) , 4.20 (s, 4H, CH_2OCH_2) , 6.68 (d, J = 7.7 Hz, 1H, Ph-H4') , 7.11 (t, J = 7.6 Hz, 1H, Ph-H5'), 7.53-7.61 (m, 2H, Ph-H2', Ph-H6'), 7.85 (s, 1H, CH), 8.81 (s, 1H, 2-NH), 12.57 (s, 1H, 9-NH); ^{13}C NMR (100 MHz, DMSO-d_6) δ: 21.9, 45.6, 66.7, 114.7, 115.9, 119.2, 121.4, 128.6, 136.5, 137.7, 142.0, 153.5, 153.8, 156.1; HRMS (ESI): calcd for $C_{16}H_{18}N_6O$ $[M+H]^+$: 311.1620, found: 311.1620. IR (KBr pellet, cm^{-1}): 3421, 3330, 2959, 2918, 2859, 1603, 1581, 1530, 1489, 1391, 1315, 1287, 1268, 1220, 1162, 1112, 1071, 1024, 941, 879, 826, 785, 729, 694, 631, 527, 443.

4.1.3.6. 6-morpholino-N-(3-(trifluoromethyl)phenyl)-9H-purin-2-amine (3g)

White solid, yield 74.1%. m.p. 209-210 ºC; ^{1}H NMR (400 MHz, DMSO-d_6) δ: 3.74 (s, 4H,

CH_2NCH_2) , 4.22 (s, 4H, CH_2OCH_2) , 7.17 (d, *J* = 7.5 Hz, 1H, Ph-*H*4'), 7.45 (t, *J* = 7.8 Hz, 1H, Ph-*H*5'), 7.88 (d, *J* = 8.0 Hz, 1H, Ph-*H*6'), 7.89 (s, 1H, C*H*), 8.37 (s, 1H, Ph-*H*2'), 9.30 (s, 1H, 2-N*H*), 12.64 (s, 1H, 9-N*H*); ^{13}C NMR (100 MHz, DMSO-d_6) δ: 31.1, 45.7, 66.7, 114.3, 115.1, 116.5, 121.9, 129.8, 136.9, 142.9, 153.3, 153.8, 155.8; HRMS (ESI): calcd for $C_{16}H_{15}F_3N_6O$ $[M+H]^+$: 365.1338, found: 365.1341. IR (KBr pellet, cm^{-1}): 3450, 3108, 2995, 2962, 2861, 1585, 1536, 1446, 1399, 1337, 1316, 1281, 1270, 1161, 1111, 1068, 1022, 937, 878, 831, 789, 724, 696, 633, 586, 525, 487.

4.1.3.7. 6-morpholino-N-(3-(trifluoromethoxy)phenyl)-9H-purin-2-amine (3h)

White solid, yield 71.6%. m.p. 201-202 ºC; ^{1}H NMR (400 MHz, DMSO-d_6) δ: 3.73 (s, 4H, CH_2NCH_2) , 4.21 (s, 4H, CH_2OCH_2) , 6.80 (d, *J* = 7.2 Hz, 1H, Ph-*H*4'), 7.33 (t, *J* = 7.9 Hz, 1H, Ph-*H*5'), 7.63 (d, *J* = 7.9 Hz, 1H, Ph-*H*6'), 7.90 (s, 1H, C*H*), 8.02 (s, 1H, Ph-*H*2'), 9.28 (s, 1H, 2-N*H*), 12.67 (s, 1H, 9-N*H*); ^{13}C NMR (100 MHz, DMSO-d_6) δ: 45.6, 66.7, 110.2, 112.2, 115.0, 117.1, 130.2, 136.9, 143.9, 149.1, 153.2, 153.8, 155.6; HRMS (ESI): calcd for $C_{16}H_{15}F_3N_6O_2$ $[M+H]^+$: 381.1287, found: 381.1277. IR (KBr pellet, cm^{-1}): 3449, 3100, 2966, 2869, 1585, 1528, 1488, 1444, 1405, 1373, 1313, 1301, 1267, 1208, 1159, 1116, 1070, 1024, 999, 960, 881, 834, 781, 772, 724, 702, 683, 632, 582, 524, 489, 446.

4.1.3.8. 2,2,2-trifluoro-N-(3-((6-morpholino-9H-purin-2-yl)amino)phenyl)acetamide (3i)

White solid, yield 66.7%. m.p. 206-207 ºC; ^{1}H NMR (400 MHz, DMSO-d_6) δ: 3.72 (s, 4H, CH_2NCH_2), 4.19 (s, 4H, CH_2OCH_2), 7.07 (d, *J* = 7.7 Hz, 1H, Ph-*H*4'), 7.25 (t, *J* = 8.0 Hz, 1H, Ph-*H*5'), 7.55 (d, *J* = 8.1 Hz, 1H, Ph-*H*6'), 7.89 (s, 1H, C*H*), 8.16 (s, 1H, Ph-*H*2'), 9.14 (s, 1H,

2-N*H*), 11.19 (s, 1H, N*H*COCF$_3$), 12.65 (s, 1H, 9-N*H*); ^{13}C NMR (100 MHz, DMSO-d_6) δ: 45.8, 66.7, 112.0, 114.1, 114.6, 116.4, 129.1, 136.6, 136.8, 142.5, 153.2, 153.7, 155.6; HRMS (ESI): calcd for $C_{17}H_{16}F_3N_7O_2$ $[M+H]^+$: 408.1396, found: 408.1387. IR (KBr pellet, cm^{-1}): 3286, 2864, 1680, 1606, 1551, 1448, 1407, 1371, 1308, 1285, 1202, 1023, 939, 880, 784, 723, 686, 610, 524.

4.1.3.9. N-(3-chlorophenyl)-6-morpholino-9H-purin-2-amine (3j)

White solid, yield 89.5%. m.p. 216-217 ºC; ^{1}H NMR (400 MHz, DMSO-d_6) δ: 3.73 (s, 4H, C*H*$_2$NC*H*$_2$) , 4.21 (s, 4H, C*H*$_2$OC*H*$_2$) , 6.88 (d, *J* = 7.7 Hz, 1H, Ph-*H*4'), 7.24 (t, *J* = 8.0 Hz, 1H, Ph-*H*5'), 7.60 (d, *J* = 8.2 Hz, 1H, Ph-*H*6'), 7.89 (s, 1H, C*H*), 8.06 (s, 1H, Ph-*H*2') , 9.17 (s, 1H, 2-N*H*), 12.69 (s, 1H, 9-N*H*); ^{13}C NMR (100 MHz, DMSO-d_6) δ: 45.7, 66.7, 115.0, 116.9, 117.6, 120.0, 130.3, 133.3, 136.8, 143.7, 153.2, 153.7, 155.6; HRMS (ESI): calcd for $C_{15}H_{15}ClN_6O$ $[M+H]^+$: 331.1074, found: 331.1072. IR (KBr pellet, cm^{-1}): 3404, 3139, 3004, 2859, 1618, 1591, 1520, 1482, 1456, 1438, 1392, 1372, 1313, 1291, 1264, 1218, 1152, 1109, 1072, 1019, 937, 874, 782, 773, 729, 689, 631, 579, 554, 528.

4.1.3.10. N-(3-fluorophenyl)-6-morpholino-9H-purin-2-amine (3k)

White solid, yield 79.0%. m.p. 210-211 ºC; ^{1}H NMR (400 MHz, DMSO-d_6) δ: 3.73 (s, 4H, C*H*$_2$NC*H*$_2$) , 4.21 (s, 4H, C*H*$_2$OC*H*$_2$) , 6.64 (t, *J* = 8.3 Hz, 1H, Ph-*H*4'), 7.25 (m, 1H, Ph-*H*5'), 7.44 (d, *J* = 8.1 Hz, 1H, Ph-*H*6'), 7.86 (s, 1H, Ph-*H*2'), 7.89 (s, 1H, C*H*), 9.18 (s, 1H, 2-N*H*), 12.67 (s, 1H, 9-N*H*); ^{13}C NMR (100 MHz, DMSO-d_6) δ: 45.6, 66.7, 104.7, 104.9, 106.5, 106.7, 114.3, 114.9, 130.1, 130.2, 136.8, 143.9, 144.0, 153.2, 153.8, 155.7, 161.7, 164.1; HRMS (ESI): calcd for $C_{15}H_{15}FN_6O$ $[M+H]^+$: 315.1370, found: 315.1372. IR (KBr pellet, cm^{-1}): 3289, 3210,

2860, 1598, 1581, 1531, 1490, 1447, 1392, 1315, 1292, 1268, 1140, 1112, 1024, 939, 866, 785, 770, 634, 531.

4.1.3.11. N-(4-fluorophenyl)-6-morpholino-9H-purin-2-amine (3l)

White solid, yield 85.2%. m.p. 264-265 ºC; ^{1}H NMR (400 MHz, DMSO-d_6) δ: 3.72 (s, 4H, CH_2NCH_2), 4.19 (s, 4H, CH_2OCH_2), 7.08 (t, J = 8.6 Hz, 2H, Ph-*H*3', Ph-*H*5'), 7.71-7.80 (m, 2H, Ph-*H*2', Ph-*H*6'), 7.85 (s, 1H, C*H*), 8.94 (s, 1H, 2-N*H*), 12.59 (s, 1H, 9-N*H*); ^{13}C NMR (100 MHz, DMSO-d_6) δ: 45.7, 66.7, 114.7, 115.1, 115.3, 120.1, 120.1, 136.5, 138.5, 153.6, 153.8, 155.7, 156.0, 158.1; HRMS (ESI): calcd for $C_{15}H_{15}FN_6O$ $[M+H]^+$: 315.1370, found: 315.1370. IR (KBr pellet, cm^{-1}): 3303, 2857, 1603, 1580, 1529, 1509, 1473, 1442, 1389, 1317, 1287, 1221, 1154, 1115, 1019, 936, 884, 832, 817, 796, 685, 655, 627, 544, 532.

4.1.3.12. 6-morpholino-N-(pyridin-3-yl)-9H-purin-2-amine (3m)

Yellow solid, yield 38.5 %. m.p. 283-284 ºC; ^{1}H NMR (400 MHz, DMSO-d_6) δ: 3.71-3.76 (m, 4H, CH_2NCH_2) , 4.10-4.30 (m, 4H, CH_2OCH_2), 7.27 (dd, J = 8.3, 4.6 Hz, 1H, Ph-*H*6'), 7.89 (s, 1H, C*H*), 8.07 (d, J = 4.6, 2.3 Hz, 1H, Ph-*H*5'), 8.20 (d, J = 8.4 Hz, 1H, Ph-*H*4'), 8.91 (d, J = 2.4 Hz, 1H, Ph-*H*2'), 9.13 (s, 1H, 2-N*H*), 12.65 (s, 1H, 9-N*H*); ^{13}C NMR (100 MHz, DMSO-d_6) δ: 45.7, 66.7, 115.0, 123.6, 124.9, 136.8, 138.7, 140.7, 141.5, 153.3, 153.8, 155.8; HRMS (ESI): calcd for $C_{14}H_{15}N_7O$ $[M+H]^+$: 298.1416, found: 298.1414. IR (KBr pellet, cm^{-1}): 3371, 2965, 2907, 2865, 2794, 2555, 1593, 1548, 1531, 1503, 1486, 1437, 1423, 1385, 1331, 1282, 1233, 1223, 1192, 1134, 1110, 1081, 1043, 1018, 932, 891, 800, 785, 700, 644, 635, 534, 518.

4.1.3.13. 5-((6-morpholino-9H-purin-2-yl)amino)picolinamide (3n)

White solid, yield 20.8%. m.p. > 300 ºC; ^{1}H NMR (400 MHz, DMSO-d_6) δ: 3.75 (m, 4H, CH_2NCH_2), 4.22 (s, 4H, CH_2OCH_2), 7.38 (s, 1H, CON*H*), 7.89 (s, 1H, C*H*), 7.94 (bs, 2H, CON*H*, Py-*H*6'), 8.40 (bs, 1H, Py-*H*5'), 8.93 (bs, 1H, Py-*H*2'), 9.51 (s, 1H, 2-N*H*), 12.74 (s, 1H, 9-N*H*); ^{13}C NMR (100 MHz, DMSO-d_6) δ: 45.7, 66.7, 115.2, 122.6, 124.4, 137.1, 138.6, 141.1, 142.1, 153.1, 153.8, 155.3, 166.7; HRMS (ESI$^-$): calcd for $C_{15}H_{16}N_8O_2$ [M-H]: 341.1474, found: 341.1473. IR (KBr pellet, cm^{-1}): 3284, 2858, 1721, 1590, 1532, 1488, 1438, 1371, 1282, 1230, 1118, 1011, 890, 857, 789, 703, 658, 567.

4.1.3.14. 6-morpholino-N-(pyrazin-2-yl)-9H-purin-2-amine (3o)

White solid, yield 16.4%.m.p. > 300 ºC; ^{1}H NMR (400 MHz, DMSO-d_6) δ: 3.74 (s, 4H, CH_2NCH_2), 4.22 (s, 4H, CH_2OCH_2), 7.94 (s, 1H, C*H*), 8.13 (s, 1H), 8.26 (s, 1H), 9.40 (s, 1H), 9.56 (s, 1H, 2-N*H*), 12.75 (s, 1H, 9-N*H*); ^{13}C NMR (100 MHz, DMSO-d_6) δ: 45.8, 66.7, 110.0, 115.4, 136.0, 136.8, 137.3, 142.6, 151.0, 153.1, 154.3; HRMS (ESI): calcd for $C_{13}H_{14}N_8O$ $[M+H]^+$: 299.1369, found: 299.1371. IR (KBr pellet, cm^{-1}): 3422, 3202, 3120, 2921, 2855, 1621, 1585, 1543, 1481, 1420, 1388, 1302, 1283, 1264, 1158, 1145, 1116, 1070, 1025, 1010, 939, 823, 787, 743, 634, 529.

4.1.3.15. N-(6-morpholino-9H-purin-2-yl)quinolin-3-amine (3p)

White solid, yield 49.2%. m.p. 246-247 ºC; ^{1}H NMR (400 MHz, DMSO-d_6) δ: 3.73-3.79 (m, 4H, CH_2NCH_2), 4.25 (s, 4H, CH_2OCH_2), 7.50-7.55 (m, 2H), 7.78 (dt, J = 6.1, 2.6 Hz, 1H), 7.88-7.92 (m, 1H), 7.93 (s, 1H, C*H*), 8.80 (d, J = 2.2 Hz, 1H), 9.07 (d, J = 2.5 Hz, 1H), 9.48 (s, 1H, 2-N*H*),

12.72 (s, 1H, 9-N*H*); ^{13}C NMR (100 MHz, DMSO-d_6) δ: 45.7, 66.7, 115.1, 118.9, 126.6, 127.2, 127.4, 128.8, 129.0, 135.9, 137.0, 143.2, 145.8, 153.3, 153.9, 155.8; HRMS (ESI): calcd for $C_{18}H_{17}N_7O$ $[M+H]^+$: 348.1573, found: 348.1573. IR (KBr pellet, cm^{-1}): 3417, 3202, 3078, 2961, 2853, 1592, 1541, 1493, 1478, 1450, 1390, 1308, 1285, 1267, 1220, 1113, 1068, 1021, 936, 880, 830, 785, 748, 639, 616, 550.

4.1.3.16. N^2-phenyl-N^6-(tetrahydro-2H-pyran-4-yl)-9H-purine-2,6-diamine (5a)

White solid, yield 67.5%. m.p. 228-229 ºC; ^{1}H NMR (400 MHz, DMSO-d_6) δ: 1.62-1.75 (m, 2H, C*H*CHC*H*), 1.83-1.92 (m, 2H, C*H*CHC*H*), 3.41 (t, *J* = 11.1 Hz, 2H, C*H*OC*H*), 3.94 (d, *J* = 10.1 Hz, 2H, C*H*OC*H*), 4.34 (s, 1H, CHC*H*CH), 6.85 (t, *J* = 7.0 Hz, 1H, Ph-*H*4'), 7.22 (t, *J* = 7.5 Hz, 2H, Ph-*H*3', Ph-*H*5'), 7.32 (s, 1H, 6-N*H*), 7.81 (s, 2H, Ph-*H*2', Ph-*H*6'), 7.84 (s, 1H, C*H*), 8.79 (s, 1H, 2-N*H*), 12.40 (s, 1H, 9-N*H*); ^{13}C NMR (100 MHz, DMSO-d_6) δ: 15.6, 33.2, 46.8, 65.4, 67.0, 118.6, 120.4, 128.7, 136.7, 142.3, 154.2, 156.7; HRMS (ESI): calcd for $C_{16}H_{18}N_6O$ $[M+H]^+$: 311.1620, found: 311.1622. IR (KBr pellet, cm^{-1}): 3429, 3332, 3126, 2957, 2847, 1604, 1537, 1477, 1441, 1374, 1327, 1241, 1164, 1138, 1085, 933, 788, 758, 638, 487.

4.1.3.17. N^2-(4-fluorophenyl)-N^6-(tetrahydro-2H-pyran-4-yl)-9H-purine-2,6-diamine (5b)

White solid, yield 67.5%. m.p. 132-133 ºC; ^{1}H NMR (400 MHz, DMSO-d_6) δ: 1.68 (d, *J* = 9.9 Hz, 2H, C*H*CHC*H*), 1.80-1.92 (m, 2H, C*H*CHC*H*), 3.40 (m, 2H, C*H*OC*H*), 3.93 (d, *J* = 10.2 Hz, 2H, C*H*OC*H*), 4.31 (s, 1H, CHC*H*CH), 7.06 (t, *J* = 8.5 Hz, 2H, Ph-*H*3', Ph-*H*5'), 7.33 (s, 1H, 6-N*H*), 7.87-7.76 (m, 3H, C*H*, Ph-*H*2', Ph-*H*6'), 8.84 (s, 1H, 2-N*H*), 12.40 (s, 1H, 9-N*H*); ^{13}C NMR (100 MHz, DMSO-d_6) δ: 15.6, 33.2, 46.8, 65.4, 66.9, 114.9, 115.1, 120.0(d), 136.7, 138.8, 154.2, 155.7,

156.7, 158.0; HRMS (ESI): calcd for $C_{16}H_{17}FN_6O$ $[M+H]^+$: 329.1526, found: 329.1534. IR (KBr pellet, cm^{-1}): 3422, 3128, 2958, 2847, 1608, 1509, 1476, 1386, 1334, 1215, 1162, 1139, 1084, 1011, 935, 829, 788, 638, 509.

4.1.3.18. 4-morpholino-N-phenylthieno[3,2-d]pyrimidin-2-amine (8a)

White solid, yield 77.4%. m.p. 179-180 ºC; ^{1}H NMR (400 MHz, DMSO-d_6) δ: 3.77 (s, 4H, CH_2NCH_2), 3.89 (s, 4H, CH_2OCH_2), 6.88 (t, J = 7.0 Hz, 1H, Ph-H4'), 7.15-7.34(m, 3H, CH, Ph-H3', Ph-H5'), 7.78 (d, J = 7.6 Hz, 2H, Ph-H2', Ph-H6'), 8.09 (d, J = 5.2 Hz, 1H, SCH), 9.10 (s, 1H, 2-NH); ^{13}C NMR (100 MHz, DMSO-d_6) δ: 46.4, 66.4, 106.5, 118.9, 120.9, 124.2, 128.8, 133.8, 141.8, 157.9, 158.5, 163.5; HRMS (ESI): calcd for $C_{16}H_{16}N_4OS$ $[M+H]^+$: 313.1121, found:313.1121. IR (KBr pellet, cm^{-1}): 3353, 3057, 2969, 2862, 1602, 1567, 1542, 1511, 1485, 1467, 1442, 1377, 1317, 1278, 1249, 1234, 1158, 1114, 1067, 1054, 1012, 996, 887, 863, 790, 709, 692, 666, 628, 556, 503.

4.1.3.19. N-(4-methoxyphenyl)-4-morpholinothieno[3,2-d]pyrimidin-2-amine (8b)

White solid, yield 83.4%. m.p. 167-168 ºC; ^{1}H NMR (400 MHz, DMSO-d_6) δ: 3.72 (s, 3H, OCH_3) , 3.73-3.79 (m, 4H, CH_2NCH_2), 3.83-3.90 (m, 4H, CH_2OCH_2), 6.86 (d, J = 9.1 Hz, 2H, Ph-H3', Ph-H5'), 7.19 (d, J = 5.5 Hz, 1H, CH), 7.65 (d, J = 9.0 Hz, 2H, Ph-H2', Ph-H6'), 8.06 (d, J = 5.5 Hz, 1H, SCH)， 8.89 (s, 1H, 2-NH); ^{13}C NMR (100 MHz, DMSO-d_6) δ: 46.4, 55.6, 66.4, 106.0, 114.1, 120.6, 124.1, 133.6, 135.0, 154.1, 158.1, 158.6, 163.6; HRMS (ESI): calcd for $C_{17}H_{18}N_4O_2S$ $[M+H]^+$: 343.1229, found: 343.1221. IR (KBr pellet, cm^{-1}): 3429, 3234, 3186, 3154, 3127, 3060, 3029, 2958, 2901, 2869, 2832, 1605, 1569, 1544, 1510, 1460, 1443, 1426, 1443, 1427,

1373, 1310, 1279, 1249, 1239, 1183, 1127, 1029, 1011, 889, 822, 790, 760, 744, 704, 667, 548.

4.1.3.20. 4-morpholino-N-(3,4,5-trimethoxyphenyl)thieno[3,2-d]pyrimidin-2-amine (8c)

White solid, yield 75.9%. m.p. 170-171 ºC; ^{1}H NMR (400 MHz, DMSO-d_6) δ: 3.61 (s, 3H, p-OCH_3), 3.73-3.80 (m, 10H, OCH_3 , CH_2NCH_2), 3.88-3.94 (m, 4H, CH_2OCH_2), 7.20 (s, 2H, Ph-*H*2', Ph-*H*6'), 7.22 (d, *J* = 5.5 Hz, 1H, C*H*), 8.09 (d, *J* = 5.5 Hz, 1H, SC*H*), 8.99 (s, 1H, 2-N*H*); ^{13}C NMR (100 MHz, DMSO-d_6) δ: 46.4, 56.1, 60.6, 66.4, 96.6, 106.3, 124.2, 132.0, 133.9, 138.0, 153.1, 157.8, 158.6, 163.5; HRMS (ESI): calcd for $C_{19}H_{22}N_4O_4S$ $[M+H]^+$: 403.1440, found: 403.1441. IR (KBr pellet, cm^{-1}): 3278, 3100, 2957, 2853, 1606, 1573, 1543, 1508, 1447, 1383, 1346, 1279, 1235, 1201, 1129, 1066, 1017, 882, 822, 790, 723, 660, 527, 471.

4.1.3.21. 4-morpholino-N-phenyl-7H-pyrrolo[2,3-d]pyrimidin-2-amine (11a)

White solid, yield 73.6%. m.p. 196-197 ºC; ^{1}H NMR (400 MHz, DMSO-d_6) δ: 3.68-3.78 (m, 4H, CH_2NCH_2), 3.79-3.89 (m, 4H, CH_2OCH_2), 6.48 (s, 1H,C*H*), 6.83 (t, *J* = 7.2 Hz, 1H, Ph-*H*4'), 6.88-6.95 (m, 1H, NHC*H*), 7.22 (t, *J* = 7.8 Hz, 2H, Ph-*H*3', Ph-*H*5'), 7.79 (d, *J* = 7.9 Hz, 2H, Ph-*H*2', Ph-*H*6'), 8.72 (s, 1H, 2-N*H*), 11.24 (s, 1H, 7-N*H*); ^{13}C NMR (100 MHz, DMSO-d_6) δ: 46.0, 66.6, 97.5, 106.6, 118.3, 119.4, 120.2, 128.7, 142.4, 154.1, 155.5, 157.5; HRMS (ESI): calcd for $C_{16}H_{17}N_5O$ $[M+H]^+$: 296.1511, found: 296.1513. IR (KBr pellet, cm^{-1}): 3337, 3199, 3122, 2994, 2852, 1593, 1571, 1531, 1497, 1474, 1427, 1365, 1306, 1279, 1248, 1167, 1110, 1073, 1013, 904, 886, 789, 750, 729, 692, 594, 520, 495.

4.1.3.22. N-(4-methoxyphenyl)-4-morpholino-7H-pyrrolo[2,3-d]pyrimidin-2-amine (11b)

Light yellow solid, yield 78.3%. m.p. 193-194 ºC; ^{1}H NMR (400 MHz, DMSO-d_6) δ: 3.71 (s, 3H, OCH_3), 3.71-3.77(m, 4H, CH_2NCH_2), 3.78-3.84(m, 4H, CH_2OCH_2), 6.46 (s, 1H, CH), 6.82 (d, J = 8.8 Hz, 2H， Ph-H3', Ph-H5'), 6.87 (s, 1H, NHCH), 7.67 (d, J = 8.8 Hz, 2H, Ph-H2', Ph-H6'), 8.50 (s, 1H, 2-NH), 11.22 (s, 1H, 7-NH); ^{13}C NMR (100 MHz, DMSO-d_6) δ: 46.0, 55.6, 66.6, 97.2, 101.6, 114.0, 119.0, 120.0, 135.8, 153.6, 154.4, 155.9, 157.5; HRMS (ESI): calcd for $C_{17}H_{19}N_5O_2$ $[M+H]^+$: 326.1617, found: 326.1618. IR (KBr pellet, cm^{-1}): 3438, 3120, 3012, 2952, 2861, 1591, 1569, 1510, 1460, 1438, 1399, 1377, 1298, 1289, 1258, 1230, 1167, 1115, 1097, 1033, 1016, 901, 882, 825, 788, 700, 592, 553, 524, 459.

4.1.3.23. 4-morpholino-N-(3,4,5-trimethoxyphenyl)-7H-pyrrolo[2,3-d]pyrimidin-2-amine (11c)

Beiges solid, yield 58.5%. m.p. 193-194 ºC; ^{1}H NMR (400 MHz, DMSO-d_6) δ: 3.60 (s, 3H, OCH_3), 3.76 (s, 10H, OCH_3, CH_2NCH_2), 3.84 (s, 4H, CH_2OCH_2), 6.48 (s, 1H, CH), 6.93 (s, 1H, NHCH), 7.22 (s, 2H, Ph-H2', Ph-H6'), 8.59 (s, 1H, 2-NH), 11.19 (s, 1H, 7-NH); ^{13}C NMR (100 MHz, DMSO-d_6) δ: 46.1, 56.1, 60.6, 66.6, 96.4, 97.5, 101.6, 131.7, 138.6, 153.1, 154.2, 155.5, 157.5; HRMS (ESI): calcd for $C_{19}H_{23}N_5O_4$ $[M+H]^+$: 386.1828, found: 386.1829. IR (KBr pellet, cm^{-1}): 3350, 2958, 2853, 1722, 1592, 1575, 1506, 1480, 1446, 1404, 1361, 1275, 1231, 1125, 1019, 901, 820, 729, 467.

4.2. Biological assay

4.2.1. In vitro CHK1 kinase assay

White 384-well polystyrene plates (#3674, Corning) and ADP-Glo kit (#V9101, Promega Corporation) were used to determine CHK1 inhibitory activities of compounds **3a-p**, **5a**, **5b**, **8a-c**

and **11a-c**. The buffer solution was prepared according to the manufacture's protocol. All the test compounds, CHK1 kinase, Cdc25 peptide and ATP were dissolved in the buffer solution. 2 μL of various concentrations of test compounds (ranging from 50 to 0.05 μM of final concentration) and 4 μL of 0.8 ng/μL CHK1 kinase solution were added per well in triplicate. After incubation for 30 min at room temperature, 4 μL of the mixture containing 0.067 mg/mL Cdc25 peptide and 30 μM ATP was added per well to give a final assay volume of 10 μL. This final assay solution was incubated for another 60 min at room temperature in dark. Subsequently, 10 μL of the ADP-Glo reagent was added to terminate the kinase reaction and deplete the unconsumed ATP. After an additional incubation for 40 min at room temperature, 20 μL of the kinase detection reagent was added to convert adenosine diphosphate (ADP) to ATP and luciferase or luciferin was introduced to detect the ATP. Chemiluminescence was measured using a plate-reading luminometer (FlexStation 3, Molecular Devices) after incubation for 40 min at room temperature in dark. IC_{50} values were calculated using Graphpad Prism software. AZD7762 and CCT245737 were used as the positive controls. Assays were performed in duplicate and repeated on separate days.

4.2.2. Cytotoxicities against HT29 cell line and Hek293 cell line

All the target compounds were screened for their cytotoxicities towards HT29 and Hek293 cells (Beijing Dingguo Changsheng Biotechnology Co. LTD) using MTS assay. Cells were seeded into 96-well plates at 3.0×10^3 cells per well in a volume of 100 μL of medium and then cultured for 36 h at 37 ºC in a humidified 5% CO_2 environment prior to treatment. Subsequently, cells were treated by 10 μM of the test compounds and incubated for 72 h. Then, 20 μL of the MTS solution (5 mg/mL in PBS) was added to each well. The optical density at 490 nm was determined by a

Benchmark Plus Microplate Reader (Bio-Rad). Three separate experiments with triplicate data were performed to obtain mean cell viability. Appropriate controls were included and the results were expressed as inhibition rates of test compounds relative to untreated controls. The GI_{50} value, which is the concentration of drug to cause 50% reduction in proliferation of cancer cells, was calculated to reflect the cytotoxicity.

4.2.3. Colony formation assay on HT29 cell line

The anti-colony formation activity of compound **3l** was evaluated against HT29 cell. HT29 cells were seeded into 6-well plates at 100 cells per well in a volume of 2 mL of medium and then cultured for 48 h at 37 ºC in a humidified 5% CO_2 environment prior to treatment. Then, the cells were treated by different concentrations of **3l** ranging from 100 nM to 100 μM for another 48 h. The medium was discarded and 2 mL of fresh medium without **3l** was added per well. Subsequently, the cells were cultured for 2 weeks. After 15 mins fixing with methanol, colonies were stained with 0.1% crystal violet and quantitated by microscope counting.

4.2.4. Antitumor potentiating assay on HT29 cell line

HT29 cells were seeded into 96-well plates at 3.0×10^3 cells per well in a volume of 100 μL medium and then cultured for 36 h at 37 ºC in a humidified 5% CO_2 environment prior to treatment. The cells treated with 40 μM of the test compounds in a volume of 50 μL to give a final concentration of 10 μM or 1 μM of **3l** and mixed for 1 min. Subsequently, 50 μL gemcitabine solution was added into each well to give the final concentrations ranging from 1.56 nM to 400 nM (8 concentrations). After mixing for 1 min, the cells were incubated at 37 ºC in a humidified

atmosphere for 72 h. The optical density at 490 nm was determined by a Benchmark Plus Microplate Reader (Bio-Rad). Three separate experiments with triplicate data were performed to obtain mean cell viability. The results were expressed as inhibition rates of test compounds relative to untreated controls. The potentiating factor (fold) was used as a measure of the ability of the test compound to enhance cytotoxicity of gemcitabine. It was calculated by the ratio of the GI_{50} of gemcitabine in combination with test compound to the GI_{50} of gemcitabine alone.

4.2.5. Cell cycle analysis

The HT29 cells (1.5×10^6 cells in 60 mm culture dishes) were treated by 10 μM of **3l** alone, 25 nM of GEM alone or 25 nM GEM in combination with 10 μM of **3l** for 48 h, respectively, in comparison to an untreated control. Then, the cells were collected, washed with ice-cold phosphate buffered saline (PBS) and fixed with ice-cold 70% ethanol overnight at 4 ºC. The next day, cells were centrifuged, the supernatant was discarded and the pellet was treated with RNase A (125μg/ml) at 37 C for 30 min in dark. The treated cells were stained with propidium iodide (50 μg/ml) for 15 min at room temperature in dark. Cells were analyzed on flow-cytometer (FACS Calibur, Becton Dickinson) and data were collected in list mode on 10,000 events. The resulting DNA distributions were analyzed by Modfit software (Verity Software House Inc.) for the proportions of cells in G1-phase, S-phase, and G2/M-phases of the cell cycle.

4.2.6. Kinase selectivity profiling

Compound **3l** was tested its inhibition against 14 kinases in the concentration of 10 μM. The kinases were expressed in Escherichia coli BL21 strain, which was infected with bacteriophage T7.

Then, the kinases were marked with DNA in Hek-293 cells. The small molecular ligands were linked with biotin and cultured with streptavidin-coated magnetic beads for 30 min. Excess concentration of biotin was used to block the ligand-coated magnetic beads. The unbound ligands were washed with blocking buffer containing Seablock (Pierce), 1% bovine serum albumin (BSA), 0.05% Tween 20 and 1 mM dithiothreitol (DTT). The test compounds were dissolved in DMSO. The DNA marked kinase, ligand-coated magnetic beads and test compounds in 1x binding buffer (20% SeaBlock, 0.17x PBS, 0.05% Tween 20, 6 mM DTT) were added subsequently into 384 well plate. After cultured on oscillator for 1 h under room temperature, the resulting ligand-coated magnetic beads were washed with washing buffer (1x PBS, 0.05% Tween 20) and eluted with elution buffer (1x PBS, 0.05% Tween 20 and 0.05 μM non-biotin affinity ligand) for 30 min. The concentration of DNA-marked kinase in the elution were measured with real-time fluorescent quantitative PCR. A positive control for each kinase was used. The results were presented as %inhibition (%Inh). The calculation of %Inh was as follow: %Inh= 100 - (test compound signal - positive comtrol signal) / (blank signal - positive control signal) ×100. The %Inh of positive control was 100. Higher value means stronger inhibition.

4.3. Molecular modeling study

The structure of **3l** was drawn and prepared as the ligand in Discovery Studio 2.5 software. The PDB (PDB code: 5F4N) file was download from Protein Bank and was prepared as the receptor in Discovery Studio 2.5 software. CDocker protocol of Discovery Studio 2.5 was used to score the docking mode of **3l** into the ATP pocket of 5F4N using the default settings. The best docked pose of **3l** was visualized in PyMol 1.6.x.

AUTHOR INFORMATION

First Author:

Chao Tian and Zifei Han are the co-first authors of this paper. They contributed equally.

Corresponding Author:

Chao Tian and Junyi Liu are co-corresponding authors of this paper. Phone: +86 15210922099.

E-mail: tianchao@bjmu.edu.cn & jyliu@bjmu.edu.cn.

Author Contributions

The manuscript was written by Chao Tian and Zifei Han. All the authors have given approval to the final version of the manuscript.

ACKNOWLEDGMENTS

This work was supported by the National Natural Science Foundation of China (21302007).

REFERENCES

[1] A. Ciccia, S.J. Elledge, The DNA damage response: making it safe to play with knives, Mol. Cell 40 (2010) 179-204.

[2] Y. Dai, S. Grant, New insights into checkpoint kinase 1 in the DNA damage response signaling network, Clin. Cancer Res. 16 (2010) 376-383.

[3] Z. Xiao, Z. Chen, A.H. Gunasekera, T.J. Sowin, S.H. Rosenberg, S. Fesik, H. Zhang, Chk1 mediates S and G2 arrests through Cdc25A degradation in response to DNA-damaging agents, J. Biol. Chem. 278 (2003) 21767-21773.

[4] J. Smith, L.M. Tho, N. Xu, D.A. Gillespie, The ATM-Chk2 and ATR-Chk1 pathways in DNA

damage signaling and cancer, Adv. Cancer Res. 108 (2010) 73-112.

[5] C.A. Clarke, P.R. Clarke, DNA-dependent phosphorylation of CHK1 and claspin in human cell-free system, Biochem. J. 388 (2005) 705−712.

[6] C.S. Sorensen, L.T. Hansen, J. Dziegielewski, R.G. Syljuasen, C. Lundin, J. Bartek, T. Helleday, The cell-cycle checkpoint kinase chk1 is required for mammalian homologous recombination repair, Nat. Cell Biol. 7 (2005) 195-201.

[7] M.D. Garrett, I. Collins, Anticancer therapy with checkpoint inhibitors: what, when and where? Trends Pharmacol. Sci. 32 (2011) 308-316.

[8] R.T. Bunch, A. Eastman, Enhancement of cisplatin induced cytotoxicity by 7-hydroxystaurosporine (UCN-01), a new G2-checkpoint inhibitor, Clin. Cancer Res. 2 (1996) 791−797.

[9] Q.Z. Wang, S.J. Fan, A. Eastman, P.J. Worland, E.A. Sausville, P.M. O'Connor, UCN-01: A potent abrogator of G2 checkpoint function in cancer cells with disrupted p53, J. Natl. Cancer Inst. 88 (1996) 956-965.

[10] S. Rundle, A. Bradbury, Y. Drew, N.J. Curtin, Targeting the ATR-CHK1 axis in cancer therapy, Cancers 9 (2017), 41.

[11] V. Oza, S. Ashwell, L. Almeida, P. Brassil, J. Breed, C. Deng, T. Gero, M. Grondine, C. Horn, S. Ioannidis, D. Liu, P. Lyne, N. Newcombe, M. Pass, J. Read, S. Ready, S. Rowsell, M. Su, D. Toader, M. Vasbinder, D. Yu, Y. Yu, Y. Xue, S. Zabludoff, J. Janetka, Discovery of checkpoint kinase inhibitor (S)-5-(3-Fluorophenyl)-N-(piperidin-3-yl)-3-ureidothiophene-2-carboxamide (AZD7762) by structure-based design and optimization of thiophenecarboxamide ureas, J. Med. Chem. 55 (2012) 5130-5142.

[12] R. Montano, I. Chung, K.M. Garner, D. Parry, A. Eastman, Preclinical development of the novel Chk1 inhibitor SCH900776 in combination with DNA-damaging agents and antimetabolites. Mol. Cancer Ther. 11 (2012) 427-438.

[13] A. Blasina, J. Hallin, E. Chen, M.E. Arango, E. Kraynov, J. Register, S. Grant, S. Ninkovic, P. Chen, T. Nichols, P. O'Connor, K. Anderes, Breaching the DNA damage checkpoint via PF-00477736, a novel small-molecule inhibitor of checkpoint kinase 1, Mol. Cancer Ther. 7 (2008) 2394-2404.

[14] C. King, H. Diaz, D. Barnard, D. Barda, D. Clawson, W. Blosser, K. Cox, S. Guo, M. Marshall, Characterization and preclinical development of LY2603618: a selective and potent Chk1 inhibitor, Invest. New Drugs 32 (2014) 213-226.

[15] C. King, H.B. Diaz, S. Mcneely, D. Barnard, J. Dempsey, W. Blosser, R.P. Beckmann, D. Barda, M.S. Marshall, LY2606368 causes replication catastrophe and antitumor effects through CHK1-dependent mechanisms, Mol. Cancer Ther. 14 (2015) 2004-2013.

[16] D. Hong, J. Infante, F. Janku, S. Jones, L.M. Nguyen, H. Burris, A. Naing, T.M. Bauer, S. Piha-Paul, F.M. Johnson, R. Kurzrock, L. Golden, S. Hynes, J. Lin, A.B. Lin, J. Bendell, Phase I study of LY2606368, a checkpoint kinase 1 inhibitor, in patients with advanced cancer. J. Clin. Oncol. 34 (2016) 1764-1771.

[17] J. Infante, A. Hollebecque, S. Postel-Vinay, T. Bauer, B. Blackwood, M. Evangelista, S. Mahrus, F. Peale, X. Lu, S. Sahasranaman, R. Zhu, Y. Chen, X. Ding, E.R. Murray, J.L. Schutzman, J.O. Lauchle, J.-C. Soria, P.M. LoRusso, Phase I study of GDC-0425, a checkpoint kinase 1 inhibitor, in combination with gemcitabine in patients with refractory solid tumors, Clin. Cancer Res. 23 (2017) 2423-2432.

[18] J.D. Osborne, T.P. Matthews, T. Mchardy, N. Proisy, K.M. Cheung, M. Lainchbury, N. Brown, M.I. Walton, P.D. Eve, K.J. Boxall, A. Hayes, A.T. Henley, M.R. Valenti, A.K. De Haven Brandon, G. Box, Y. Jamin, S.P. Robinson, I.M. Westwood, R.L.van Montfort, P.M. Leonard, M.B. Lamers, J.C. Reader, G.W. Aherne, F.I. Raynaud, S.A. Eccles, M.D. Garrett, I. Collins, Multiparameter lead optimization to give an oral checkpoint kinase 1 (CHK1) inhibitor clinical candidate: (R)-5-((4-((Morpholin-2-ylmethyl)amino)-5-(trifluoromethyl)pyridin-2-yl)amino)pyrazine-2-carbonitrile (CCT245737), J. Med. Chem. 59 (2016) 5221-5237.

[19] M.I. Walton, P.D. Eve, A. Hayes, A.T. Henley, M.R. Valenti, A.K. De Haven Brandon, G. Box, K.J. Boxall, M. Tall, K. Swales, T.P. Matthews, T. McHardy, M. Lainchbury, J. Osborne, J.E. Hunter, N.D. Perkins, G.W. Aherne, J.C. Reader, F.I. Raynaud, S.A. Eccles, I. Collins, M.D. Garrett, The clinical development candidate CCT245737 is an orally active CHK1 inhibitor with preclinical activity in RAS mutant NSCLC and Eμ-MYC driven B-cell lymphoma, Oncotarget 7 (2016) 2329-2342.

[20] N. Sakurikar, A. Eastman, Will targeting Chk1 have a role in the future of cancer therapy? J. Clin. Oncol. 33 (2015) 1075-1077.

[21] E. Sausville, P. LoRusso, M. Carducci, J. Carter, M.F. Quinn, L. Malburg, N. Azad, D. Cosgrove, R. Knight, P. Barker, S. Zabludoff, F. Agbo, P. Oakes, A. Senderowicz, Phase I dose-escalation study of AZD7762, a checkpoint kinase inhibitor, in combination with gemcitabine in US patients with advanced solid tumors, Cancer Chemother. Pharmacol. 73 (2014) 539-549.

[22] B. Laquente, J. Lopezmartin, D. Richards, G. Illerhaus, D.Z. Chang, G. Kim, P. Stella, D. Richel, C. Szcylik, S. Cascinu, G.L. Frassineti, T. Ciuleanu, K. Hurt, S. Hynes, J. Lin, A.B. Lin, D.

Von Hoff, E. Calvo, A phase II study to evaluate LY2603618 in combination with gemcitabine in pancreatic cancer patients, BMC Cancer 17 (2017) 137.

[23] C.R. Coxon, E. Anscombe, S.J. Harnor, M.P. Martin, B. Carbain, B.T. Golding, I.R. Hardcastle, L.K. Harlow, S. Korolchuk, C.J. Matheson, D.R. Newell, M.E. Noble, M. Sivaprakasam, S.J. Tudhope, D.M. Turner, L.Z. Wang, S.R. Wedge, C. Wong, R.J. Griffin, J.A. Endicott, C. Cano, Cyclin-dependent kinase (CDK) inhibitors: structure–activity relationships and insights into the CDK-2 selectivity of 6-substituted 2-arylaminopurines, J. Med. Chem. 60 (2017) 1746-1767.

[24] A. Thorarensen, M.E. Dowty, M.E. Banker, B. Juba, J. Jussif, T. Lin, F. Vincent, R.M. Caerwinski, A. Casimiro-Garcia, R. Unwalla, J.I. Trujillo, S. Liang, P. Balbo, Y. Che, A.M. Gibert, M.F. Brown, M. Hayward, J. Montgomery, L. Leung, X. Yang, S. Soucy, M. Hegen, J. Coe, J. Langille, F. Vajdos, J. Chrencik, J.-B. Telliez, Design of a Janus kinase 3 (JAK3) specific inhibitor 1-((2S,5R)-5-((7H-Pyrrolo[2,3-d]pyrimidin-4-yl)amino)-2-methylpiperidin-1-yl)prop-2-en-1-one (PF-06651600) allowing for the interrogation of JAK3 signaling in humans, J. Med. Chem. 60 (2017) 1971-1993.

[25] F. Musumeci, A.L Fallacara, C. Brullo, G. Grossi, L. Botta, P. Callandro, M. Chiariello, M. Kissova, E. Crespan, G. Maga, S. Schenone, Identification of new pyrrolo[2,3-d]pyrimidines as Src tyrosine kinase inhibitors in vitro active against Glioblastoma, Eur. J. Med. Chem. 127 (2017) 369-378.

[26] M.F. Koehler, P. Bergeron, E. Blackwood, K.K. Bowman, Y.-H. Chen, G. Deshmukh, X. Ding, J. Epler, K. Lau, L. Lee, L. Liu, C. Ly, S. Malek, J. Nonomiya, J. Oeh, D.F. Ortwine, D. Sampath, S. Sideris, L. Trinh, T. Truong, J. Wu, Z. Pei, J.P. Lyssikatos, Potent, selective, and

orally bioavailable inhibitors of the mammalian target of rapamycin kinase domain exhibiting single agent antiproliferative activity, J. Med. Chem. 55 (2012) 10958-10971.

[27] J.M. Murray, Z.K. Sweeney, B.K. Chan, M. Balazs, E. Bradley, G. Castanedo, C. Chabot, D. Chantry, M. Flagella, D.M. Goldstein, R. Kondru, J. Lesnick, J. Li, M.C. Lucas, J. Nonomiya, J. Pang, S. Price, L. Salphati, B. Safina, P.P. Savy, E.M. Seward, M. Ultsch, D.P. Sutherlin, Potent and highly selective benzimidazole inhibitors of PI3-kinase delta, J. Med. Chem. 55 (2012) 7686-7695.

[28] P.Y. Michellys, B. Chen, T. Jiang, Y. Jin, W.S. Lu, T.H. Marsilje, W. Pei, T. Uno, X. Zhu, B. Wu, T.N. Nguyen, B. Bursulaya, C. Lee, N. Li, S. Kim, T. Tuntland, B. Liu, F. San, A. Steffy, T. Hood, Design and synthesis of novel selective anaplastic lymphoma kinase inhibitors, Bioorg. Med. Chem. Lett. 26 (2016) 1090-1096.

[29] T.P. Matthews, S. Klair, S. Burns, K. Boxall, M. Cherry, M. Fisher, I.M. Westwood, M.I. Walton, T. McHardy, K.M. Cheung, R. Van Montfort, D. Williams, G.W. Aherne, M.D. Garrett, J. Reader, I. Collins, Identification of inhibitors of checkpoint kinase 1 through template screening, J. Med. Chem. 52 (2009) 4810-4819.

[30] C. Wong, R.J. Griffin, I.R. Hardcastle, J.S. Northen, L.Z. Wang, B.T. Golding, Synthesis of sulfonamide-based kinase inhibitors from sulfonates by exploiting the abrogated SN_2 reactivity of 2,2,2-trifluoroethoxysulfonates, Org. Biomol. Chem. 8 (2010) 2457-2464.

[31] H.Q. Zhang, Z. Xia, A. Vasudevan, S.W. Djuric, Efficient Pd-catalyzed synthesis of 2-arylaminopyrimidines via microwave irradiation, Tetrahedron Lett. 47 (2006) 4881-4884.

[32] B. Yang, M.M. Vasbinder, A.W. Hird, Q. Su, H. Wang, Y. Yu, D. Toader, P.D. Lyne, J.A. Read, J. Breed, S. Ioannidis, C. Deng, M. Grondine, N. DeGrace, D. Whitston, P. Brassil, J.W. Janetka,

Adventures in scaffold morphing: discovery of fused ring heterocyclic checkpoint kinase 1 (CHK1) inhibitors, J. Med. Chem. 61 (2018) 1061-1073.

[33] S.B. Koh, A. Courtin, R.J. Boyce, R.G. Boyle, F.M. Richards, D.I. Jodrell, CHK1 inhibition synergizes with gemcitabine initially by destabilizing the DNA replication apparatus, Cancer Res. 75 (2015) 3583-3595.

Highlights

1. A series of 2,6(4)-disubstituted-*9H*-purine, -thieno[3,2-*d*]pyrimidine or -*7H*-pyrrolo[2,3-*d*]pyrimidine analogues were synthesized as novel CHK1 inhibitors.

2. Most of our compounds displayed moderate to high inhibition toward CHK1 kinase and low anti-proliferative potencies against HT29 and Hek293 cells.

3. Compound **3l** exhibited strong CHK1 inhibition, high potentiation effect on the anti-proliferative activity of gemcitabine, strong effect on the cell cycle distribution of the gemcitabine-treated HT29 cells and acceptable kinase selectivity profile.